S2-Glass Fiber Reinforced Polymer Composite Based Front Bumper Simulation and Analysis to Study its Energy Absorption Behavior.

MSc. THESIS

By

Getachew Eyasu Kassaw

MASTER'S PROGRAM IN MATERIAL'S SCIENCE AND ENGINEERING

FACULTY OF MECHANICAL AND INDUSTRIAL ENGINEERING

ETHIOPIA INSTITUTE OF TECHNOLOGY

MEKELLE UNIVERSITY (MEKELLE, TIGRAY)

MARCH 2026

S2-Glass Fiber Reinforced Polymer Composite Based Front Bumper Simulation and Analysis to Study its Energy Absorption Behavior.

A THESIS

Submitted in partial fulfilment of the requirements for the award of a degree

of

MASTERS SCIENCE

in

MATERIAL'S SCIENCE AND ENGINEERING

by

GETACHEW EYASU KASSAW

Under supervision

of

GOITOM TESFAYE (Ph.D.)

Advisor

MASTER'S PROGRAM IN MATERIAL SCIENCE AND ENGINEERING

FACULTY OF MECHANICAL AND INDUSTRIAL ENGINEERING

ETHIOPIA INSTITUTE OF TECHNOLOGY

MEKELLE UNIVERSITY (MEKELLE, TIGRAY)

MARCH 2026

DECLARATION

I declare that this thesis entitled "S2-Glass Fiber Reinforced Polymer Composite Based Front Bumper Modeling and Analysis to Study It's Energy Absorption Behavior" has been carried out by me under the guidance and supervision of advisor Dr. **Goitom Tesfaye**, Faculty of Mechanical and Industrial Engineering, Department of Material's science and engineering. I assure that the thesis proposal is made by me.

As an advisor, and to the best of my knowledge, this is to assure that the above declaration made by the candidate is correct. Therefore, as per the requirements for the award of the MSc in Materials Science and Engineering, this thesis work is complete. The guidance and all sources of materials used for the thesis have been properly acknowledge.

Candidate's name	**Signature**	**Date**
Getachew Eyasu		**25th March 2026**
Advisor's Name		
Dr. Goitom Tesfaye (Ph.D.)		17th March, 2026

THESIS ACCEPTANCE APPROVAL FORM

This is to certify that **Mr. Getachew Eyasu Kassaw** has incorporated all comments forwarded by the internal and external examiners and the chairperson during the thesis defense.

Members of the Examination Board

Mr. Redae Alemayehu (MSc.)		March 24/2026
Name of Chairman	Signature	Date
Eshete Kassegn (Ph.D.)		17th March, 2026
Name of the Internal Examiner	Signature	Date
Belay Brehane (Ph.D.)		March, 17/2026
Name of the External Examiner	Signature	Date

Confirmation

Head of the Postgraduate and Research Office

Fana Filli		
Head Name	Signature	Date

Faculty of Mechanical and Industrial Engineering (FoMIE)

Michael G/yesus (PhD)		
Dean Name	Signature	Date

ACKNOWLEDGEMENT

First and foremost, I express my gratitude to the **Almighty God** for his unending love and assistance. **Dr. Goitom Tesfaye** my advisor deserves my gratitude and appreciation for guiding me through my thesis proposal work and supporting me in my thoughts. I appreciate his detailed instruction on the review and technique, which enabled me to develop a coherent understanding of the literature and quickly write this thesis proposal.

Finally, I want to express my gratitude to all of those who have supported me in many ways and encouraged me to continue my work.

ABSTRACT

Road safety is a major concern in the automotive industry, as accidents continue to endanger human life and impose significant socio-economic costs. Vehicle bumpers, as a primary component of the restraint system, play a critical role in absorbing crash energy and reducing the transmission of impact forces to the vehicle body and passengers. Conventional steel bumpers, however, are limited in their ability to absorb energy efficiently, motivating the need for alternative lightweight, high-strength materials with superior crashworthiness.

This study investigates the design and analysis of an Epoxy S-2 Glass Fiber bumper with a fiber-to-matrix volume ratio of 60:40, intended to replace the conventional steel bumper in the TOYOTA COROLLA SEDAN (2009-2019) model. In this study the optimal polymer composite bumper material having highest priority vector score of 1.8 was evaluated by using Analytical hierarchy process(AHP). The proposed composite bumper was designed by using SOLIDWORK and analyzed under a 40 km/h frontal collision using finite element simulations in ANSYS explicit dynamics. The crashworthiness of the bumper is evaluated mainly in terms of internal energy absorption behavior.

The simulation results show that the composite bumper absorbs 865 J of total internal energy, corresponding to approximately 73.8% of the initial kinetic energy being dissipated through structural deformation of the bumper components, and with a specific energy absorption of 86.5 J/kg based on the combined mass of the bumper beam and supporting energy-absorbing plates. Literature reports indicate that energy absorption for similar composite bumper impact tests ranges from approximately 41.2 J to 96.5 J, confirming that the obtained specific energy absorption falls within expected values. Enhanced energy absorption reduces the force transmitted to the chassis, thereby lowering the risk of structural damage and improving passenger protection during collisions.

The findings demonstrate that Epoxy S-2 Glass Fiber bumpers are a promising replacement for conventional steel bumpers, offering better crash performance, improved energy absorption, and reduced vehicle damage while contributing to lightweight and safer automotive structures.

Key words; Automotive Bumper, Composite Material, Energy Absorption, Crashworthiness.

TABLE OF CONTENTS

Contents

ABBREVIATIONS

PEI - Poly Either Imide.

GF-RP – Glass Fiber-Reinforced Plastic

GMT – Glass Mat Thermoplastic

FMVSS - Federal Motor Vehicle Safety Standards.

COR - Coefficient Of Restitution.

AHP - Analytical Hierarchy Process.

FG - Functionally Graded.

FGF- Functionally Graded Foam Filled.

SMC - Sheet Molding Compound.

IIHS - Insurance Institute for Highway Safety.

NASS - National Automotive Sampling System

GAD - General Area of Damage

DOF - Direction Of Force

NOMENICLATURES

E_{11} – Young's modulus in first in-plane principal direction of fiber.

E_{22} - Young's modulus in second in-plane principal direction of fiber

v - In plane Poisson's ratio

G_{12} - Shear modulus in-plane

G_{13}- Shear modulus through thickness

G_{23} - Shear modulus through thickness

V_f - Volume fraction of the fiber

V_m - Volume fraction of the matrix

Δm - Matrix elongation

δ_f - Fiber elongation

LIST OF FIGURES

LIST OF TABLES

CHAPTER ONE

1 INTRODUCTION

1.1 Background of the study

A bumper is an automotive shield that installed on the front and back of the car and can be made of metals, plastics and composites. The bumper system absorbs the impact energy during collusion to avoid or reduce the vehicle parts(radiator, exhaust systems, hoods and feeders headlights) and passenger's damage. The safety of the passengers during vehicle crashes can be ensured to a certain limit by using good bumpers (Habtamu 2017).

When low-weighing materials are used in place of the current materials and the bumper system is optimized to improve structural energy absorption and reduce weight, the bumper system will have a high application potential.

The bumper beam is expected to be deformable enough to absorb the impact energy to protect occupants from injury, and it should possess sufficient strength and stiffness to protect its nearby components simultaneously. additionally, the increasing need for environmental protection and energy conservation has driven weight reduction in car manufacturers.

From the overall car crashes, about 60% of the crash occur at the front of the vehicle and the other oblique, side, rear side of vehicle crashes are less frequent (Jacob and Arunkumar 2016).

Figure 1, Shows the arrangements of how the actual full frontal impact and front corner impact tests were conducted (Sonawane and Shelar 2018). The configuration during these tests is:

For the full frontal test configuration, the height of the barrier was 457 mm from the ground to the lower edge of the barrier a vehicle speed of 10 km/h, and for the front corner test configuration, the height of the barrier was 406 mm from the ground to the lower edge of the barrier a vehicle speed of 5 km/h.

a) b)

Figure 1 a) Real view of the front bumper of a car. b) Central and corner impacts (Sonawane and Shelar 2018)

Numerous attempts have been employed by researchers during the lightweight design process, such as material replacement and the structural optimization method. A lot of works has been conducted to replace the heavy metallic materials with lightweight materials such as aluminum alloy, magnesium alloy, and fiber-reinforced plastic composite with high specific strength and high specific stiffness properties for improving fuel economy and structural safety. Therefore, the composite materials have been recently considered as one of the excellent candidate materials to develop automotive components, such as a bumper beam. As one class of typical composite materials, glass fiber reinforced plastic (GFRP) has been widely used to reduce the weight of a bumper beam (Zhu, Wang et al. 2017).

Figure 2 Shows the schematic view of the vehicle's front structure, which mainly includes the outer plastic bumper, crush brackets, and metal bumper. This arrangement shows the plastic bumper acts as the bumper cover, which protects from the low-speed impacts or the initial impacts, and the metal bumper acts as the bumper beam to protect low and high-speed impacts. Bumpers of colliding vehicles should lineup geometrically so that they engage each other during a low and high-speed crash to absorb crash or impact energy. Bumpers should stay engaged with the other bumpers in collisions instead of overriding or under-riding them, which often results in damage to headlights, fenders, hoods, and trunks. Bumpers should have sufficient energy-absorbing capabilities to cone damage to the bumper system itself (Sonawane and Shelar 2018).

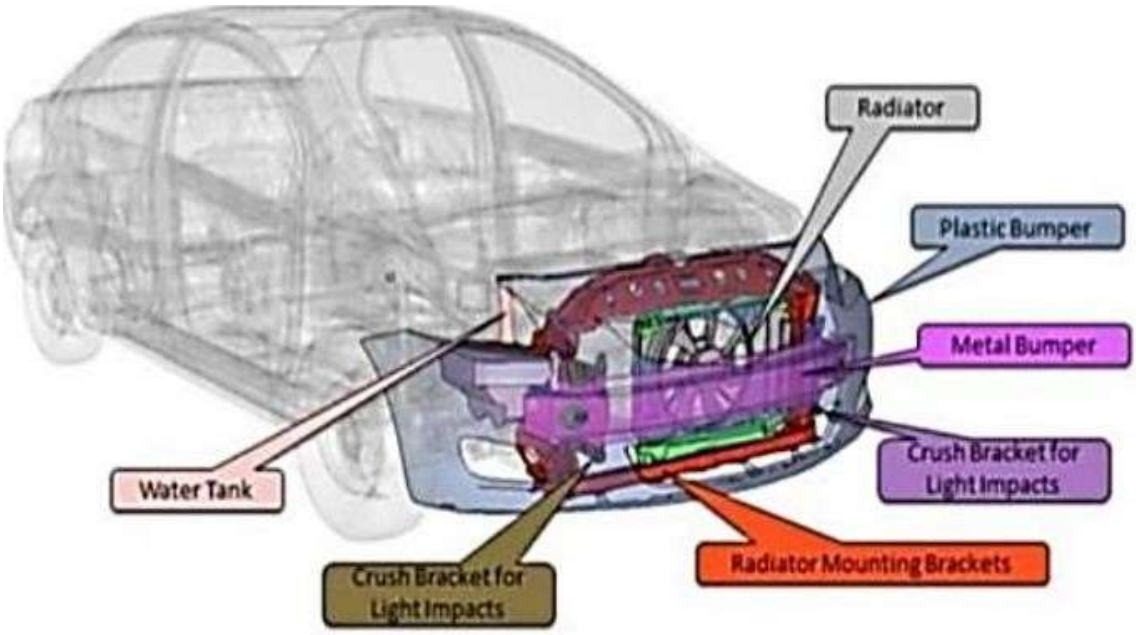

Figure 2. Diagram of the automobile front structure (Sonawane and Shelar 2018)

In order to improve the bumper beam's capacity to absorb energy in the event of a frontal collision, a hybrid composite bumper beam composed of glass fiber epoxy composite and carbon fiber epoxy composite was studied. Additionally, it was studied if the steel pads fastened to the of the bumper beam might enhance energy absorption capacity by crushing the front two tires of automobiles (Cheon and Choi 1995).

Basic requirements for bumper material include

- Adequate kinetic energy absorption
- High strength
- good corrosion resistance
- Lightweight
- Low cost simple to manufacture in huge quantities

Composite materials can attract the researcher's because they are lightweight and have good mechanical properties (Dixit, Begeman et al. 2017). However, material failure results from the abrupt change in properties at the junction during the delamination process. A novel kind of type of composite material called functionally graded material was created to address this significant problem(Olorunnishola and Adubi 2018). The main difference between functionally graded

materials and composite materials are that the properties of composite materials uniform throughout, whereas the properties of a functionally graded material vary along their volume, length, thickness, and other factors (Zhang, Khan et al. 2019).

In addition to offering durability, corrosion resistance, toughness, design flexibility, resilience, and great performance at a cheap cost, composites are now primarily utilized to reduce weight and increase energy efficiency in automobiles. In order to design the new car bumper constructed of S2 glass fiber reinforced epoxy resin, this study uses ANSYS software. The impact cases are then determined by utilizing FEM to assess the stress concentration distribution.

1.2 Statement of the problem

The problem with the front bumper of a light-duty vehicle is that the material of the bumper is being made. Traditional steel and aluminum bumpers provide limited energy absorption and require higher structural mass to achieve crash performance. In contrast, composite bumper systems can absorb 50–60% more collision energy, exhibit 60–70% lower deformation, and are significantly lighter 40–50% lighter than steel. Although, Designers are still working to improve the bumper beam requirements (mainly energy absorption and performance), further improvements are needed to enhance customer safety and vehicle safety issues. Although they used low-velocity impact testing, previous research studies have shown that a significant amount of stress absorption occurs as a result of impact modifications in the bumper's cross-section. Low-speed impact tests are primarily used for recyclable materials that are readily dented or deformed since we now need to investigate the consequences of applying high-velocity impact towards the impactor.

The problem for predicting the composite’s complex behavior (anisotropic, orthotropic) before fabrication is solved using computer-aided design and analysis software's.. Thus, ANSYS software, which stands for computer-aided design and analysis, eliminates the need for expensive trials and enables the optimization of parts prior to manufacturing. Composite materials are increasingly being used in the automobile components industry due to their favorable mechanical, physical, thermal, and energy-absorbing qualities. Therefore, the goal of this effort is to replace such traditional front bumpers with composite materials and examine the properties that will affect them.

1.3 Objectives of the study

1.3.1 General objective of the study

The general objective of this study was to simulate and analyze the energy absorption behavior of an S2-glass fiber reinforced polymer composite-based front bumper under impact loading conditions.

1.3.2 Specific objectives of the study

The specific objectives of the study were:

- To model the S2-glass fiber reinforced polymer composite front bumper using CAD software.
- To perform finite element simulation of the bumper under a 40 km/h frontal impact condition.
- To evaluate the energy absorption, deformation, and stress distribution of the bumper using FEM analysis.
- To assess the structural behaviors of the S2-glass fiber composite bumper based on simulation results.

1.4 Scope of the study

The energy absorption, performance, customer safety, and limitations of the current design was the primary focus of the study. This study was also focused on simulation-based analysis and provided numerical foundations for energy absorption and performance using stress-strain and energy curves that was generated from FEM software.

Finally, this document was recommend that the automotive manufacturer create and implement the design for the intended function. However, the research was limited to simulation-based analysis and provided a foundation for future prototype fabrication and experimental validation. Further experimental investigations were suggested to overcome the current scope limitations and to enhance the overall reliability and applicability of the study.

1.5 Significance of the study

The significance of this paper was to study bumper system energy absorption behavior, performance and ensure the practical advantages. Unlike studies that focused solely on mechanical behavior, this research integrated material selection criteria with practical manufacturing considerations, thereby offering a more industry-oriented framework for bumper design in light-duty passenger vehicles.

The primary beneficiaries of this research were automotive manufacturers, design engineers, and material suppliers. Automotive manufacturers could apply the findings to select composite materials that effectively balance crash performance with production feasibility. Design engineers benefited from the comparative evaluation of six composite systems, which provided guidance for optimizing bumper beam designs under impact loading. Material suppliers and fabricators could better align their products with automotive safety and performance requirements.

Furthermore, the study contributed to improved occupant safety by enhancing the understanding of energy absorption in composite bumper systems. Improved impact energy management reduced force transmission to the vehicle structure and occupants during collisions, thereby potentially lowering repair costs and minimizing economic losses for vehicle owners and insurers.

CHAPTER TWO

2 LITERATURE REVIEW

Various studies demonstrate that the bumper beam's ability to fulfill its intended design is directly impacted by the material selection, the geometric model's cross section, the thickness, the beam's curvature, and other optimization techniques.

2.1 Existing materials used for bumpers

In this section, several numerical and experimental analyses of different previously published journals have been revised. Furthermore, different materials used for constructing automotive front bumper have been revised including numerical studies. Different materials have varied impacts on beam deflection, impact force, stress distribution, and energy absorption.(Olorunnishola and Adubi 2018) discusses that Composite bumper absorbs more collision energy than steel bumper and the materials they discussed are as follows within their description.

(Hosseinzadeh, Shokrieh et al. 2005) designed a commercial front bumper beam using glass mat thermoplastic (GMT). Their research highlighted the drawbacks of conventional materials like steel and aluminum, noting issues such as structural failure and increased weight. When compared to conventional bumpers, Glass Mat Thermosetting (GMT) showed excellent impact behavior. However, due to manufacturing issues and the weight of the ribs was increased, and they were replaced by appropriate Sheet Molding Compound (SMC). Figure 3 shows the 3D structure of an SMC bumper beam modeled using LS-DYNA ANSYS 5.7, and the thickness of these local zones was maximized to strengthen the structure.

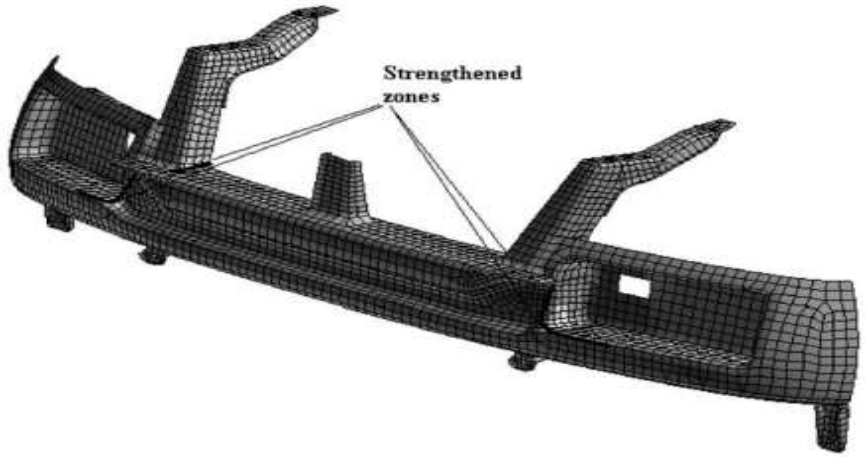

Figure 3. SMC bumpers (Hosseinzadeh, Shokrieh et al. 2005)

(Wang and Li 2015) investigated how changing the material and thickness could improve crashworthiness performance in low velocity impacts while also reducing the weight of the bumper beam. They also performed bumper beam analysis on carbon fiber composite and steel materials to determine deformation, weight, impact force, energy absorption, and impact acceleration. As a result, the carbon fiber composite bumper beam performs better under impact. To achieve a lightweight design, bumper beams with various thicknesses (5.4, 6, 6.6, and 7.2mm) were analyzed. The findings indicate that the 5.4mm beam offers the optimal choice without compromising impact performance. Based on stress distribution analysis, the thickness distribution of the bumper beam was adjusted to enhance weight reduction. The results show that the optimized design further decreases the overall weight while maintaining impact resistance.

(Osokoya 2017) studied that steel is the most often used material in bumper beam due to its high strength, stiffness, moderate energy absorption capabilities, corrosion resistance and fatigue performances. Aluminum is also utilized for bumper beams because of its lightweight and lower cost than steel. The off-weighting features aid in fuel economy and, as a result, pollution reduction. The use of plastic bumpers allows for a great deal of aesthetic flexibility. Plastics were once primarily used for fascia, but they are now more commonly employed as plastic reinforcing beams. Common materials for car bumper (figure 4.) with their manufacturing process had studied to evaluate nylon-6-nanoclay nanocomposite beam.

a) Steel bumper beam b) Aluminum bumper beam

c) Plastic bumpers

Figure 4. Materials used for bumper beam (Osokoya 2017)

(Marzbanrad, Alijanpour et al. 2009) designed a bumper beam using various materials including steel, magnesium, aluminum, glass mat thermoplastic (GMT), and high-strength sheet molding compound (SMC) and evaluated their performance against the above key criteria through software-based simulations. In contrast, glass mat thermoplastic (GMT) bumper beams maximize elastic strain energy and perform well in terms of deflection, impact force, and stress distribution. However, due to its high weight and production problems, glass mat thermoplastic can be replaced with a modified sheet molding compound (SMC).

(Xiao, Fang et al. 2015) designed functionally graded foam-filled bumper beam. They used three point bending test as a simulated (figure 5) and experimental test. FE models of both hollow and foam-filled bumper beams with foam fillers were simulated (Figure 6), showing that the foam-filled design provides notable energy absorption and reduces weight. Finally, the functionally graded foam-filled (FGF) bumper beam was compared to a hollow steel bumper beam. One sort of foam filled bumper is a uniform foam filled construction, while the other is a functionally

graded one with increasing density as you get closer to the center. Due to the propagation of wave energy, this offers a better response for its application and a cost-effective means of optimization. The materials employed in this design were steel and aluminum foam. Their findings revealed that the FGF bumper beam can prevent hazardous local bending behavior and has a higher energy absorption capacity.

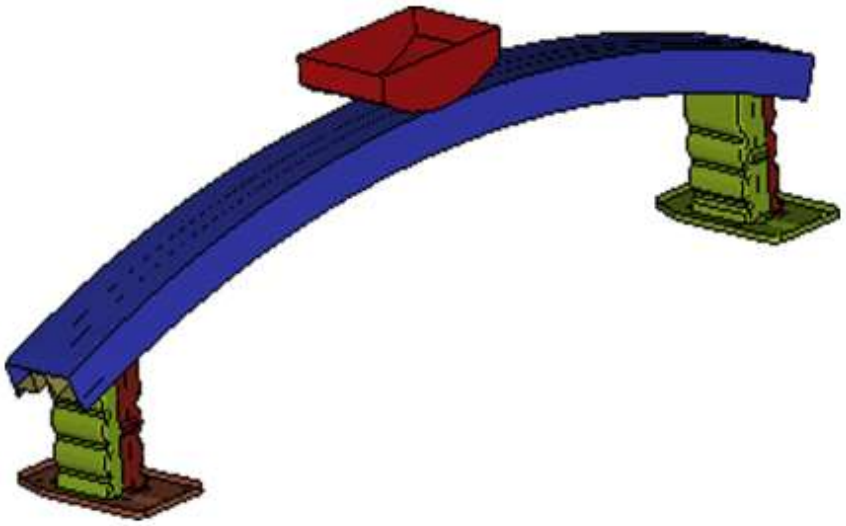

Figure 5 Three point bending simulation of bumper beam (Xiao, Fang et al. 2015)

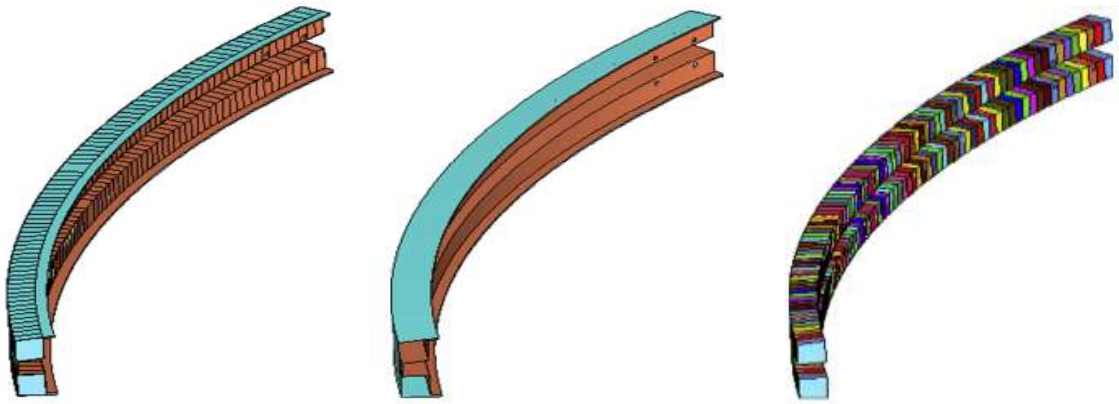

a) FGF filled bumper beam b) Empty (non foam filled) c) FGF-filler

Figure 6 FE models of hollow and foam filled bumper beam (Xiao, Fang et al. 2015)

(Bilal Abdullah Baig et al, 2015) designed a typical new front bumper beam for passenger cars using GMT composite materials. This bumper absorbs impact energy through deformation or

redirects it perpendicular to the impact direction using a spring mechanism that can convert approximately 80% of the kinetic energy into spring potential energy during low-speed collisions, meeting American standards. The bumper's design is based on aerodynamic shapes and the frontal configuration of passenger vehicles. The spring system was optimized using a Genetic Algorithm implemented in MATLAB V6. The CATIA model of the bumper was imported into LS-DYNA and ANSYS for analysis, employing nonlinear explicit impact simulation. Figure 7 illustrates the main components of conventional bumper systems.

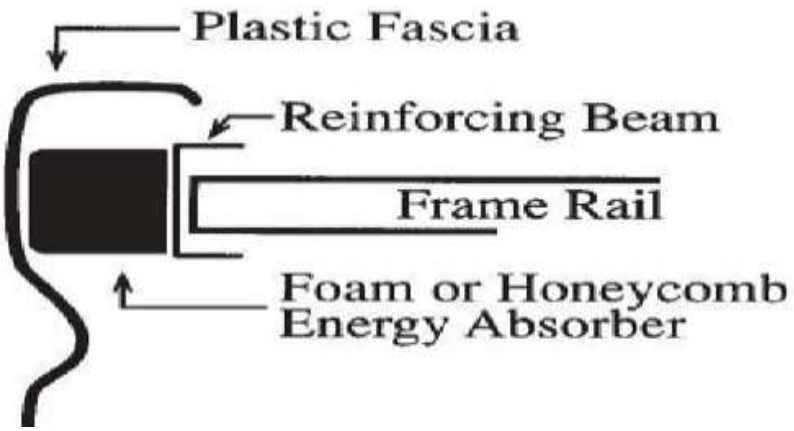

Figure 7 Configuration of common bumper type

The main elements of desired bumper are shown in figure 8.

1. Front rubber tape: that is composed of polypropylene (PEP) for damping of poor contacts.
2. Fascia: it indicates the aerodynamic form of the bumper and is used as a bearing for spring system retainer.
3. Spring system: it contains vertical springs for converting the kinetic energy to the spring potential energy and horizontal springs for connecting the fascia to base plate.
4. Conics and base plate: are main elements of the bumper for energy absorbing in high speed contacts.
5. Connecting plastic parts: two propylene (PEP) parts that connect the bumper base plate to the car.

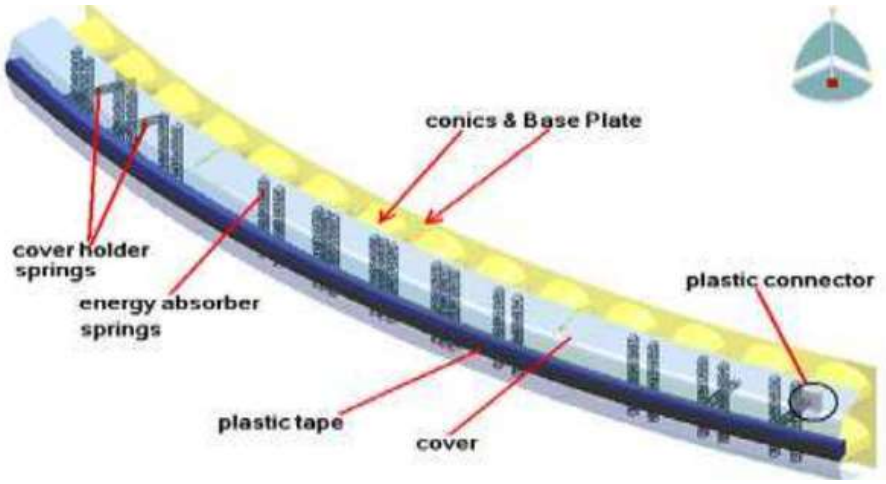

Figure 8. Schematic configuration of the desired bumper

(MOTGI, KULKARNI et al.) analyzed the front bumper of an existing passenger car in the Indian market and use impact analysis to recommend design improvements. They came to the conclusion that, from a safety perspective, the bumper is a crucial component of an automobile. Therefore, bumper analysis will help to improve passenger safety, and new bumper sizes and shapes may be considered to replace the current ones. To ascertain the deflection and plastic strain induced in the bumper beam, they modeled a front bumper beam (figure 9) and performed an impact analysis.

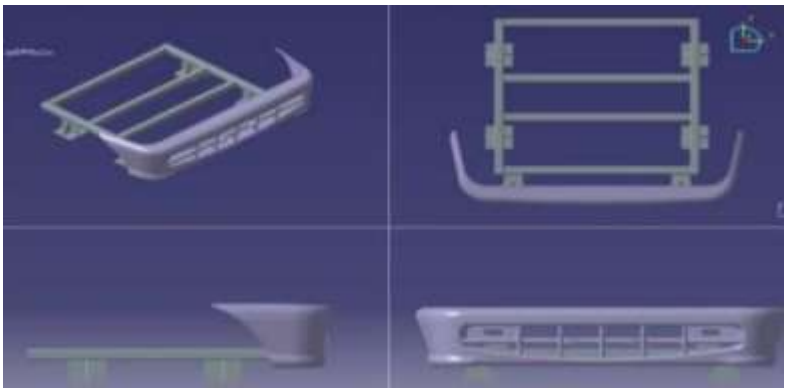

Figure 9. Front Bumper Structure (MOTGI, KULKARNI et al.)

(Madarapu and Mohan) studied key factors such as material, structure, shape, and impact conditions to analyze and improve the crashworthiness of bumper beams during collisions. The bumper simulation involved impact modeling using Pro/Engineer, while impact analysis was

performed in SOLIDWORKS at a speed of 13.3 m/sec (48 km/h), aligning with Federal Motor Vehicle Safety Standards (FMVSS) 208 for occupant crash protection. The analysis was conducted both at this regulated speed and at varying speeds to assess performance. Finite Element Analysis software was used for material simulation, and the 3D bumper model (Figure 10) was created in SOLIDWORKS. The materials evaluated for the bumper included ABS plastic and S-glass epoxy.

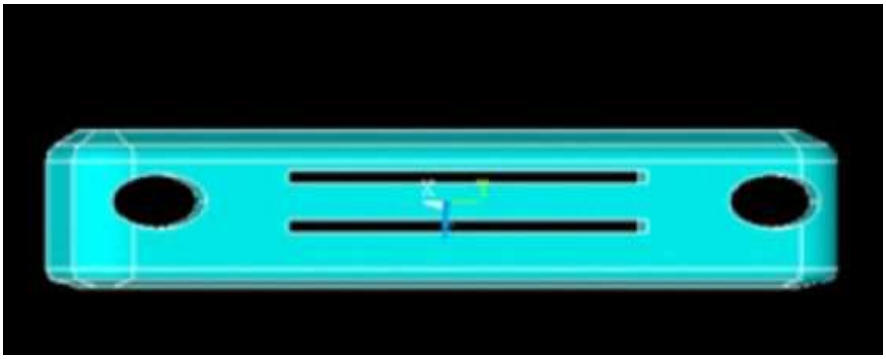

Figure 10. Model of a Car Bumper (Madarapu and Mohan)

(Nachippan, Alphonse et al. 2021) conducted a finite element modeling study of car bumpers made from polymer matrix hybrid composites reinforced with E-glass and jute fibers, both in the form of randomly oriented chopped fibers (Figure 11). The research focused on finding an alternative to the conventional pure plastic bumper material. Simulation results revealed that epoxy polymer exhibited minimal displacement under load, while urea formaldehyde showed significantly greater displacement under the same conditions. The study concluded that urea formaldehyde is unsuitable for use as a car bumper material, whereas epoxy polymer is a promising matrix material for polymer composites that could serve as an alternative bumper material.

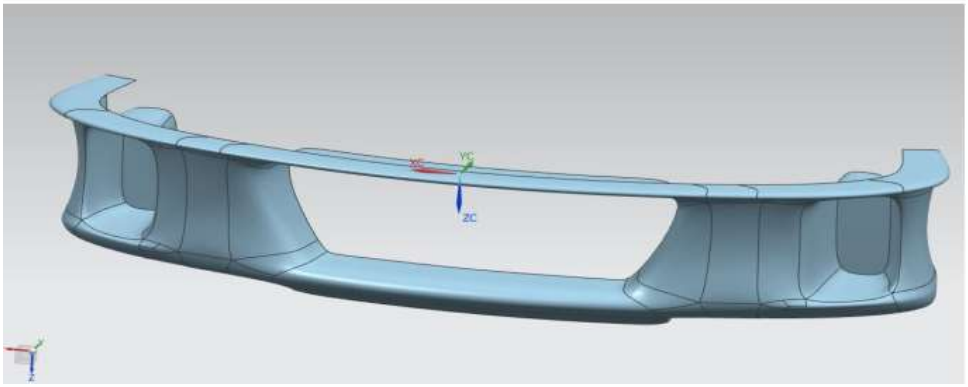

Figure 11. Car bumper model (Nachippan, Alphonse et al. 2021)

Common Materials for Car Bumpers

- Steel Bumpers
- Aluminum Bumpers
- Plastic bumpers Polymer
- composites for bumper beams
- Carbon fiber epoxy Glass fiber epoxy

(Priyatam and Madhav 2018) the front bumper and its components (figure 12) were modeled using CREO software, and a bumper beam made of three different materials (steel, composite, and honeycomb) was analyzed using ANSYS. On their work, a honeycomb type bumper beam response less deformation and less weight than the other two types.

Figure 12. Bumper beams with honey comb (Priyatam and Madhav 2018)

(Sonawane and Shelar 2018) studied slow-speed impact tests following IIHS regulations at three different points: central impact, left corner impact, and right corner impact. They analyzed parameters such as bumper material, shape, thickness, and impact conditions using finite element analysis (FEA) to improve crashworthiness in low-speed collisions. Based on their findings, modifications were made to the vehicle's front structure, revealing that aligning the front metal bumper with appropriate stiffness yields the best performance.

Generally, we see that material selection, geometrical optimization, including thickness and shape improvement, are mentioned in the literature as ways to increase energy absorption. The majority of the factors used to select materials were weight and thickness.

2.2 Effects of fiber orientation angles

Fibers that are not positioned exactly perpendicular to the fracture plane tend to enhance toughness more effectively; however, fibers aligned at steeper angles show reduced toughening due to increased fiber breakage and de-bonding (Norman and Robertson 2003). Furthermore, delamination's forming within the reinforcing layers were observed to result from matrix cracking on the underside of the composite (Davallo, Pasdar et al. 2010). In three-point bending tests, hand-lay-up composite samples with 0/90° and 0/45° fiber orientations using both glass and graphite fibers were evaluated. The 0/45° lay-up configuration demonstrated higher flexural strength compared to the 0/90° arrangement for the same fiber type (Rathnakar, Shivanand et al. 2013). The strength, rigidity, and load carrying capability of glass/epoxy with a 0^o orientation are greater than those of any other orientation (Ahmed, Kumar et al. 2013). Bidirectional glass fibers' flexural strengths at $0\text{-}90^o$ and $-45+45^o$ were compared in an experiment to determine the impact of fiber positioning on that property. The findings show that the $-45+45^o$ orientation had higher strength (Yarlagaddaa and Ramakrishna 2019). Tensile tests and bending tests for fiber orientation at 0°, 30°, 45°, 60°, and 90° angles were conducted and discussed. The behavior of these compounds was investigated using the finite element method and software called ANSYS V.13. The results showed that both extension and deflection values were highest at a 0° fiber orientation and progressively decreased as the fiber angle increased, reaching a minimum when the fibers were oriented perpendicular to the applied stress. (Abd-Ali and Madeh 2016) studied the tensile properties of glass fiber/epoxy laminates by preparing and testing appropriate

specimens. The study focused on tensile strength, tensile modulus, specific tensile strength, and specific tensile modulus. Additional data on specific tensile properties were calculated and presented in table 1. The findings indicated that fiber-reinforced polymer laminates exhibit greater strength and stiffness along the longitudinal direction compared to other orientations.

Table 1. Tabulation of tested results

Orientation Angles [Degree]	***Specimen Number***	***Tensile Strength [MPa]***	***Tensile Modulus [GPa]***	***Specific Tensile Strength [$GPam^3Kg^{-1}$]***	***Specific Tensile Modulus [$MPam^3Kg^{-1}$]***
0	1	324.42	10.07	5.529	0.171
	2	326.92	10.07	5.572	0.171
45	1	47.71	2.53	0.813	0.0431
	2	49.40	2.53	0.842	0.0431
90	1	37.81	1.55	0.466	0.026
	2	22.40	2.32	0.381	0.039

2.3 Summary of previous works reported in literature

Several studies have focused on the design, analysis, and material selection for lightweight automotive bumper beams, particularly in enhancing impact performance and reducing weight.

(Osokoya 2017) evaluated polymer composites and found that carbon fiber/epoxy composites offer a higher specific tensile strength than traditional materials like steel and aluminum. Similarly, glass fiber-reinforced composites showed competitive specific tensile strength compared to these metals. (Priyatam and Madhav 2018) analyzed and optimized bumper beams using steel, composite, and honeycomb structures, concluding that honeycomb-based bumpers provide reduced deformation and weight, making them suitable for heavy vehicles.

(Sonawane and Shelar 2018) conducted slow-speed impact tests at various bumper positions center, left, and right and observed that aligning the front metal bumper with appropriate stiffness yielded optimal performance. (Wang and Li 2015) emphasized that modifying the material and thickness of carbon fiber composite bumpers can significantly enhance crashworthiness during low-velocity impacts.

(MOTGI, KULKARNI et al.) reviewed design improvements for passenger car bumpers in India, suggesting that changes in size, shape, and material based on impact analysis can lead to better impact resistance. (Olorunnishola and Adubi 2018) conducted a comparative analysis of hybrid composite bumpers made from a blend of natural jute and glass fibers versus conventional synthetic composites. Their findings highlighted the potential of hybrid configurations like HYBRID Cs, PNFC, and GF-C for automotive applications.

(Marzbanrad, Alijanpour et al. 2009) explored the role of material type, thickness, geometry, and impact conditions in bumper design. They found that optimizing these parameters improves crash performance in low-speed collisions. Likewise, (Hosseinzadeh, Shokrieh et al. 2005) developed a bumper beam using glass mat thermoplastics (GMT), which showed superior impact behavior compared to conventional bumper materials.

(Abd-Ali and Madeh 2016) examined the influence of fiber orientation on the tensile properties of glass fiber/epoxy laminates. Their results demonstrated that fiber-reinforced polymer composites exhibit significantly greater strength and stiffness along the 0° (longitudinal) direction than at other orientations, underscoring the importance of fiber alignment in composite bumper design.

2.4 Research gap of previous studies

In recent years, significant research has been conducted on the development of lightweight polymer composite materials for automotive bumper beam applications. Numerous studies have investigated the mechanical performance, impact behavior, and energy absorption characteristics of glass fiber, carbon fiber, and hybrid composite systems.

Advanced numerical simulations and experimental analyses have also been employed to optimize fiber orientation, stacking sequence, and reinforcement architecture for improved crash performance.

Despite these advancements, several limitations remain in the existing literature. Many previous studies focus predominantly on mechanical performance while giving limited attention to the combined evaluation of performance, cost, manufacturability, and material availability

Researchers design metal based bumpers like high strength steel, Aluminum B390 alloy, Chromium coated mild steel and magnesium. Even though, steel material has good mechanical properties than other material like aluminum and magnesium, its density was high. Other studied a design glass mat thermoplastic (GMT) that may replace metal bumpers while preserving its mechanical qualities and weighing less. However, due of its weight, this material was replaced with a high-strength sheet molding compound (SMC). Many other researchers was design a bumper beam with composite material. When contrasted to the materials described above, these materials can fit into the bumper system. However, these cannot be reached in terms of the

bumper beam's performance, which was required due to its serious application. Due to this, further studies have been conducted to design carbon fiber composite bumper beam. This material, among other types of composite materials, offers good strength, weight, and corrosion resistance. However it too expensive. Functionally graded (FG) materials where designed with their in particular, offer significant weight savings and great energy absorption. However, because of the way its set up, the steel metal was exposed to the accident first, and then the impact load was transferred to the foam substance. This causes the material to deform more and the stress value to rise. Finally, researchers was developed a priority ranking for the bumper materials by doing pair wise step by step comparisons of material properties and their result shows that glass fiber (E glass and S glass) reinforced polymer composite based bumper offers significant weight savings and great energy absorption. Despite the fact that E-fiberglass offers a better balance between performance and cost, strength and stiffness, studies reveals that S glass was superior in terms of resistance to chemicals, moisture, and heat. Limited works had been done on the design and developments of glass fiber (E glass and S glass) reinforced polymer composite based bumper. However, they are still rare and do not address all facets on absorption energy, performance improvements and methods of analysis. In Ethiopia, exceeding or riding beyond the speed limit frequently results in collisions with other vehicles or structures and causes higher risk of death. Analysis has been performed at low speed impacts with vertical and horizontal beam structures, as well as different front vehicles (fully or sided). However, based on risk of injury (Stucki, Ragland et al. 1995) for serious and higher injuries, the "full barrier like" impactor testing mechanism was best.

In general, a systematic evaluation that simultaneously considers energy absorption capability, structural performance, economic feasibility, manufacturing compatibility, and supply chain availability is still required. Addressing this gap contributes to a more practical and industry-oriented framework for selecting optimal polymer composite materials for automotive bumper beam applications.

Therefore, S2-glass fiber reinforced polymer composite based front bumper at 40 km/h speed impact with rigid barrier wall structure impactor was simulated and analyzed to study its energy absorption behaviors.

CHAPTER THREE

3 MATERIALS AND METHODS

3.1 MATERIALS

The material was selected using the Analytical Hierarchy Process (AHP) technique. According to the authors, the recommended approach is an effective instrument that may be used to create more realistic and stable work. Materials with more balance solutions on performance, energy absorption, weight, ease of manufacturing, service conditions, and cost. Based on this, S2-glass fiber-reinforced epoxy resin material was chosen. Despite the fact that E-fiberglass offers a better balance between performance and cost, strength and stiffness, the AHP approach reveals that S2-glass is superior in terms of resistance to chemicals, moisture, and heat. Compared to other types of polymeric composite bumpers, this S2-glass fiber reinforced epoxy resin composite material offers good energy absorption capabilities.

3.1.1 Material selection, design parameters and specifications

3.1.1.1 Impact barrier specification

According to IIHS, for all bumper simulation tests the impact barrier with 1524 mm length, 152 mm wide, and 50 mm deep aligned vertically or horizontally is simulated. At the impact, the vehicle bumper centerline is aligned forward most portion of the barrier centerline. When the impact tests are performed the barrier and vehicle should be under control. The conditions are:

- The impactor should have effective mass and fixed in all directions.
- The barrier is at rest and on rigid level.
- The vehicle engine is operating at user defined speed.
- The vehicle systems that are not necessary to the movement of the vehicle are not operating during impact.

Conditions for bumper test:-

- The impact is assumed to be central.
- No air resistance to the motion of the load, P
- The bumper systems used is assumed to be made of the same material (S2 glass epoxy resin composite material, in this case), hence, same material properties.
- No friction at contact point of the vehicle and the impact load.
- Consideration is made of a fixed bumper with an applied frontal pressure (impact load).

3.1.1.2 Specification of the car

The sample of car for TOYOTA COROLLA SEDAN (2009-2013) model to be studied by of research was specified here below according to (https://www.QEFIRA.com accessed online) and the specifications of vehicle system that are necessary to the movement of the vehicle was tabulated in table2.

Figure 13. TOYOTA COROLLA SEDAN (2009-2013) model *https://www.edmunds.com*

Table 2. Specifications of TOYOTA COROLLA SEDAN (2009-2013) model

S/N	Parameter	Value	Unit
1.	Power	132	HP
2.	Engine Size	1.8	L
3.	Cylinder	4	
4.	Driver Train	Front driver	
5.	Length	4539	Mm
6.	Width (front)	1530	Mm
7.	Height	1466	Mm
8.	Gross Weight	1740	Kg

3.1.1.3 Specification of impact speed

The maximum allowed speed on a road in optimal circumstances is known as the speed limit. Even though the speed limit rule allows for adaptation to local circumstances, Art. 84 (1) of Regulation No. 208/2011(Eshetu 2019) is still unclear due to the 1969 speed limit regulation's enforceability. In addition, the speed limit law needs to be amended because it has been in place for fifty years.

According to domestic low of FDRE the (maximum) speed limits are for urban roads 60 kph and for rural roads 70 kph and minimum speed limits are below 40 Kph. Nevertheless, for GPS integrated devices federal traffic agency on meeting the standard test approved that for private vehicles 100 kph, for rental vehicles 80kph and for heavy vehicles 70 kph for road signal of 120 kph. In Ethiopia, road traffic accidents are major challenges with various aspects of causes with lack of management and policy on the safety of road. Even though there are no formal national government-regulated draft programs to improve traffic efficiency and lower road traffic accidents, the number of traffic accidents has been rising over time. Poor road safety and

ignorance of traffic safety, particularly with regard to speed limits, are the leading causes of traffic accidents (UN Economic Commission for Africa, 2020). According to the (global economy, 2019), the road quality is low here in Ethiopia having the quality rate of 3/7. Singapore have the highest-ranking rate of 6.5/7. So for this work the speed of the car for the impact is selected among the speed ranges 40-70 kph.

3.1.1.4 Specification of impact mode

The original investigation focused on "offset" frontal hits as a possible accident scenario for simulation in accordance with the performance standards of FMVSS No.208 for full frontal impacts. The exposure population for several frontal hits or accidents was evaluated using the NASS from 1988 to 1996. In order to describe the outcome of occupant harm, the impact or collision conditions for a future frontal offset test are equally important. The following concerns, however, are also now being addressed by the agency: what are the appropriate circumstances for a full frontal test procedure in FMVSS No. 208, collinear, car-to-car crash testing at 50%, 60%, and 70% partial overlaps, and a half overlap 30 degree oblique car-to-car collision (Abrate 2011).

The NASS-CDS files from 1988 to 1996 are stated for collision or impact events that response crash pulses, which are represented by the full barrier crash pulse and are henceforth referred to as "barrier-like." Drivers of automobiles in collisions with "barrier-like" impact conditions are compared to drivers of automobiles in all frontal collisions. Vehicle drivers in "barrier-like" crashes are proportionately more likely to be engaged in frontal car-car collisions.

Comparing injury risk reveals that vehicles involved in frontal car-to-car incidents have a slightly greater injury risk for moderate and more serious injuries than those classified as "full barrier like" (7.6 percent and 6.8 percent, respectively). However, the "full barrier like" categories have the highest injury rate (3.8 percent) for more severe and serious injuries (Stucki, Ragland et al. 1995).

Most people agree that the FMVSS standards work similarly to the UN's regulations. [GlobalAutoRegs] When a car complies with the safety standards established by the UN and FMVSS, these rules are extremely beneficial regardless of the organization. Among the nations that disregard UN norms is Ethiopia.

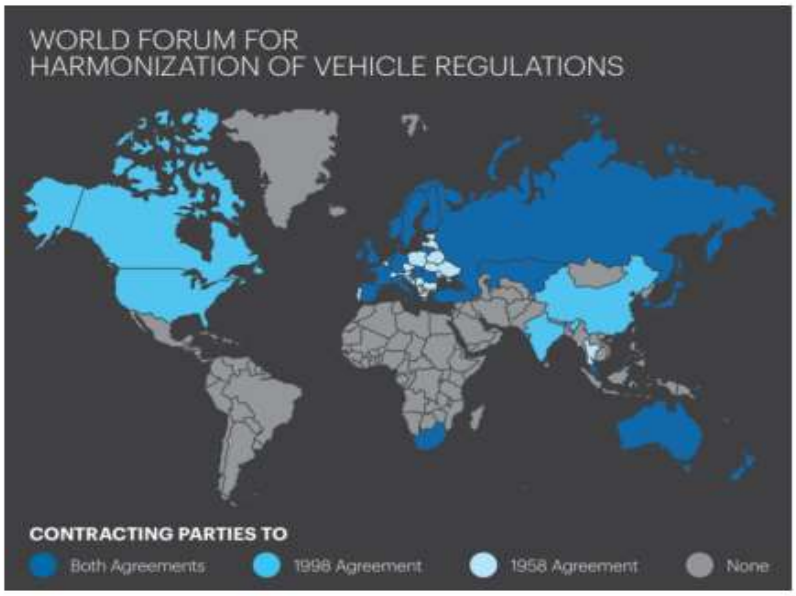

Figure 14. Countries following the UN regulations.

3.2 METHODS

The following diagram is the general road map of the project.

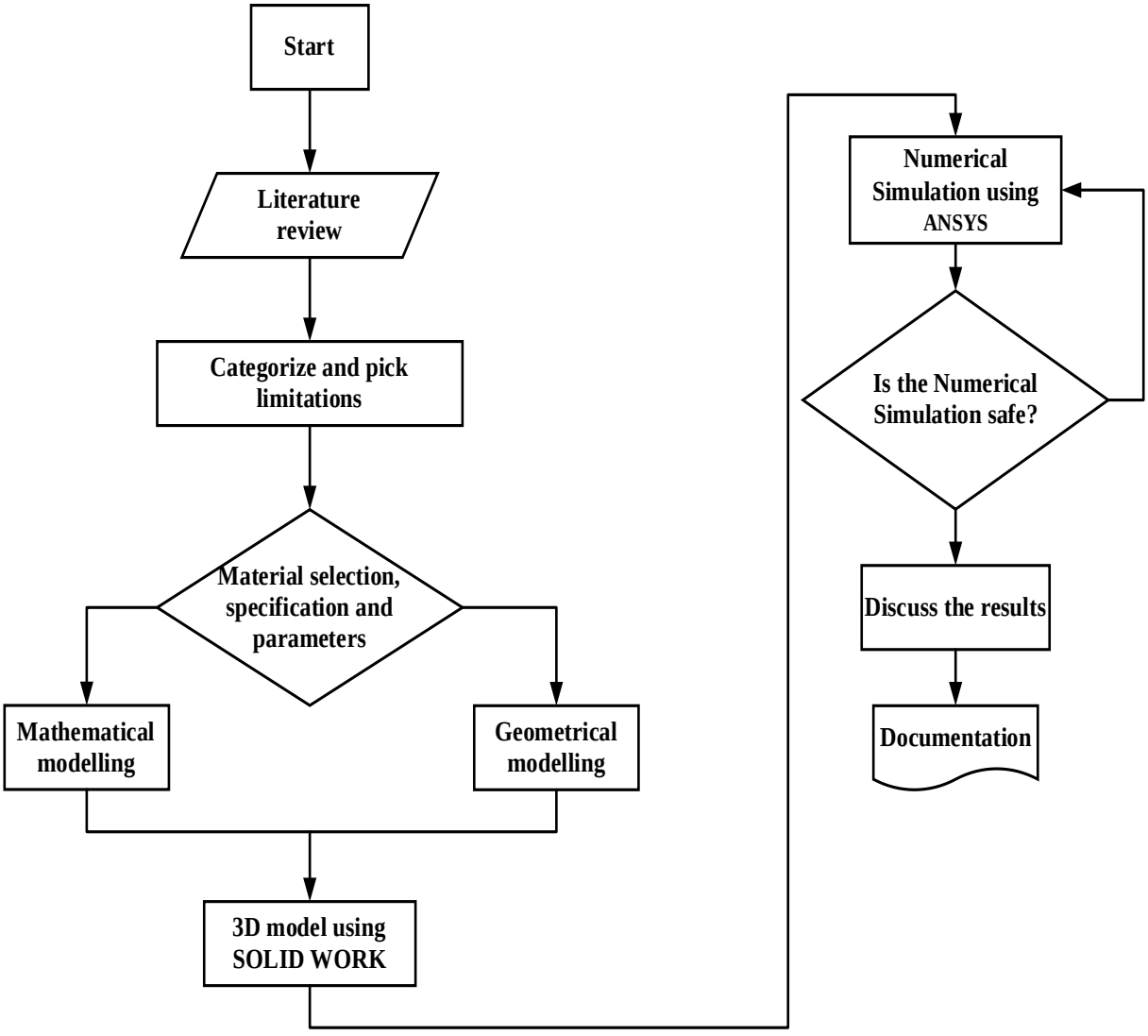

Figure 15. Road map of the methodology

3.2.1 Data collection

Data collection has been conducted in order to get important and valuable information. Above and beyond using research articles and the internet (accessed online), I have asked some Toyota Corolla car owners and spare part seller employees. I also tried to execute random unstructured interviews for drivers in the city of Mekelle to get information about driving speeds and their possibility of crash accident occurrence, but they did not know much about the bumper systems. I anticipated that respondents might not be able to participate because of their restricted free time; thus, telephone interviews were inevitable.

Due to time limitations and the availability of respondents, the interviews were conducted in an informal and unstructured manner, mainly through short face-to-face conversations and telephone discussions. No written questionnaires or signed forms were used; however, key technical questions related to vehicle speed, crash occurrence, bumper performance, and material behavior were discussed with the participants. The consultation involved three professionals with experience in automotive engineering, vehicle maintenance, and manufacturing. Their backgrounds included mechanical engineering, automotive systems, and vehicle service operations.

Observations were also made through physical inspection of vehicle bumper components and by reviewing information available on automotive parts websites. This phase was important because it provided practical insights into the structure, materials, and design considerations of front bumper systems.

3.2.2 Concept Design of the polymeric composite automotive bumper

Researchers and designers create a variety of polymeric composite automotive bumper concepts due to increasingly using composite materials to meet growing market demands for high-quality products at competitive prices. Selecting the appropriate material is critical, and composite materials have gained significant attention for automotive components, particularly bumper systems. Bumper systems typically consist of four main components: fascia, energy absorber, and beam. Among these components, the bumper beam is crucial for absorbing impact energy and safeguarding the vehicle. As such, In the automotive sector, selecting the appropriate material for

the bumper beam is crucial. To design any type of product there may be many alternatives. Due to that, this design project has also many options. In order to prepare compatible polymeric composite automotive bumper conceptual designs are developed from six alternatives.

3.2.2.1 Design Concept criteria's for selection of Polymer Composite Bumper Materials

The selection of a suitable polymer composite material for a car bumper beam is governed by multiple interrelated criteria that ensure structural safety, economic feasibility, and manufacturability. The following five criteria determine which material is best for the polymeric composite car bumper beam.

Energy absorption:-One of the most critical parameters is energy absorption capability. Since the bumper beam is a primary energy-absorbing component during low- to medium-speed impacts, materials with high specific energy absorption are preferred. Optimizing fiber orientation and fiber volume fraction plays a significant role in maximizing energy dissipation. Additionally, incorporating crushable foam cores or honeycomb structures within the composite design can further enhance impact energy absorption while maintaining low weight.

1. **Performance** requirements are equally important in the selection process. The material must meet structural strength and stiffness demands under impact and static loading conditions. High-modulus reinforcements such as carbon fibers significantly improve stiffness and load-carrying capacity. The reinforcement architecture, including woven, chopped, or unidirectional fiber arrangements, must be carefully selected to ensure effective load distribution and resistance to deformation.
2. **Cost considerations** strongly influence material selection, especially in mass-produced automotive applications. The overall cost includes raw materials, processing techniques, tooling, and labor. Efficient material utilization and waste minimization strategies help reduce production costs. Furthermore, cost-effective manufacturing processes such as hand lay-up, compression molding, or injection molding are advantageous for large-scale production.
3. **The manufacturing method** must be compatible with the selected material system. Tooling design, curing cycles, molding parameters, and automation potential all affect production efficiency and quality consistency. Production volume and lead time are also decisive

factors, particularly in the automotive industry where high throughput and repeatability are essential.

4. **Availability** is another practical consideration. The selected material system must have a stable supply chain to ensure consistent quality and timely production. Access to skilled labor, appropriate tooling, and established manufacturing facilities further supports successful implementation. Reliable partnerships with material suppliers and manufacturers reduce the risk of supply disruptions.

3.2.2.2 Design concepts

Based on the above five parameters the following six material options are generated.

Material-1: Glass Fiber Reinforced Polypropylene (GFRP-40%)

Glass Fiber Reinforced Polypropylene (GFRP-40%) represents a lightweight and durable solution widely used in automotive components. It offers good impact resistance and is compatible with standard automotive paint systems. Its energy absorption capacity is good and adequate for low-speed impacts. Although its stiffness and strength are moderate compared to carbon fiber systems, it meets general structural requirements. Injection molding enables efficient high-volume production, keeping costs low and availability excellent, making it suitable for mass-market vehicles.

Material-2: Glass Fiber Vinylester SMC (60%)

Glass Fiber Vinylester Sheet Molding Compound (GFRP-60%) provides enhanced strength and dimensional stability due to the vinyl ester resin matrix. Compared to traditional polyester systems, it offers improved mechanical properties and better resistance to chemicals and weathering. Its energy absorption is good, and structural performance surpasses standard glass-polyester composites. The SMC process allows relatively efficient production, though the cost is moderate and availability is fair compared to polypropylene-based systems.

Material-3: Carbon Fiber Reinforced Epoxy (CFRE)

Carbon Fiber Reinforced Epoxy (CFRE) delivers exceptional strength-to-weight ratio and superior stiffness, making it ideal for high-performance and racing vehicles. Its energy absorption is excellent, and it provides outstanding impact protection while significantly reducing vehicle

weight. However, advanced manufacturing methods such as autoclave molding increase production complexity and cost. Due to high material expenses and limited supply, its availability is restricted, making it less suitable for large-scale commercial vehicles but highly attractive for premium applications.

Material-4: Carbon Fiber Reinforced Polypropylene (CFRP-10%)

Carbon Fiber Reinforced Polypropylene (CFRP-10%) combines the strength benefits of carbon fiber with the flexibility and recyclability of polypropylene. While its energy absorption is moderate compared to epoxy-based carbon systems, it offers good structural performance at a more reasonable cost. Injection molding allows faster production cycles compared to thermoset carbon composites. Its cost and availability are moderate, positioning it as a balanced option between performance and manufacturability.

Material-5: Glass Fiber Reinforced Epoxy (GFRE)

Glass Fiber Reinforced Epoxy (GFRE) offers a strong combination of strength, stiffness, and durability. With excellent energy absorption and mechanical performance, it is suitable for both high-performance and general automotive applications. Manufacturing methods such as hand lay-up or vacuum infusion provide flexibility in production, although cycle times may be longer than injection molding. The cost is moderate, and availability is generally good due to the widespread use of glass fibers and epoxy resins.

Material-6: Glass Fiber Reinforced Polyester (GFRP-30%)

Glass Fiber Reinforced Polyester (GFRP-30%) is one of the most commonly used composite systems due to its balance of strength, weight, and affordability. Its energy absorption is fair, and its mechanical properties are moderate compared to epoxy-based systems. It can be manufactured using hand lay-up or molding processes with relatively low complexity. With moderate cost and good availability, it remains a practical option for cost-sensitive automotive applications.

Table 3 Material data used for choosing best material for automotive polymers bumpers

Material	ITH/ (J/cm)	FS/ MPa	Fm/ GPa	RMC/ (USD/kg)	DS/ (kg/m3)	SH	Am
M−1	7.52	294	11.4	1	1560	High	Available
M−2	12.80	427	17.9	3	1900	High	Available
M−3	10.6	656	34.5	6	1600	High	Available
M−4	3.2	75.8	13.8	5	1110	High	Available
M−5	21.2	483	20.7	4	1400	High	Available
M−6	8.54	179	11	2	1850	High	Available

3.2.2.3 Design Concept selection process and its criteria

In order to select the best alternatives and ranking the alternatives, pairwise comparison is very important. During the selection of design alternatives for all about six options, There are several ways for defining the process of deciding conceptual designs, according to (Prabhu, Chaudhari et al. 2018), decision-making is defined as an alternative of the most suitable choices for the predefined criteria.

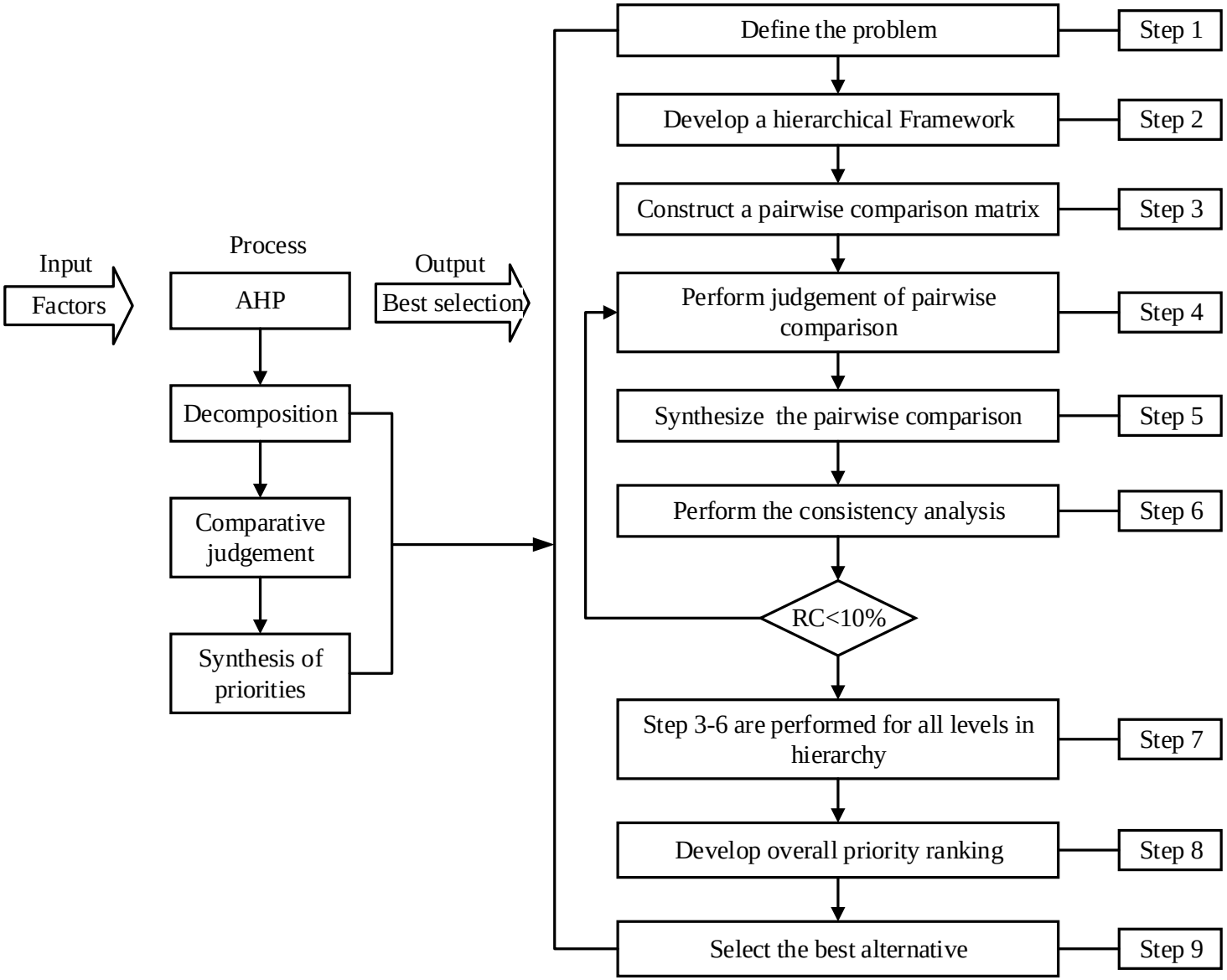

Figure 16: The steps of the analytical hierarchy process (AHP)

Step 1. Problem definition

The polymeric composite automotive bumper issues is used as a main topic. Following an examination of numerous articles on a polymeric composite automotive bumper, six alternative designs were developed. Six ideas (M-1, M-2, M-3, M-4, M-5 and M-6) are evaluated for selection based on the type of materials.

Thus, the analytical hierarchy process about the physical properties of polymeric composite automotive bumper must be used to select the most invaluable design concept.

Step 2. Develop a Hierarchy Model

Based on (Prabhu, Chaudhari et al. 2018) principal AHP has been developed in response to the terrible lack of a standardized, simply comprehensible process to facilitate the collection of complex judgment. The following valuable criteria are used to select the best option; energy absorption, performance, manufacturing method, cost, and availability are important factors to consider.

Step 3. Pair-wise matrix construction

The use of pair-wise comparison to derive precise ratio scale priority is one of AHP's most well-known accomplishments. Then, without using sublevel criteria, a pair-wise comparison matrix of size 5×5 is construct.

Table 4: pair-wise comparison scale

Relative	Definitions (value)	Explanation
1	Equal	The two requirements have equal values
3	Slightly more	One slightly favors over the another requirement
5	Strong value	One strongly favors over the another requirement
7	Very strong	A necessity is strongly favored, and its supremacy in practice is proved.
9	Extreme value	The evidence that favors one side over the other is of the greatest grade of confirmation.
2, 4, 6, and 8	Intermediates values between two adjacent judgments	Compromise
Reciprocals	For inverse comparisons	

Step 4. Pair-wise compassion judgments

The pair-wise criteria starts with a comparison of two elements' relative significance. To build the collection of matrices, $n \times (n-1)$ decisions are necessary. The authors experience and wisdom are used to make the decisions. The energy absorption (E_A) is more essential than cost in a pairwise process comparison scale (C). For every pairwise comparison in the first columns, the reciprocals of the first raw are automatically allocated.

Table 5: Pairwise comparison of criteria concerning in concept design

Criteria	Energy absorption	performance	Manufacturing method	cost	Availability
Energy absorption	1	3	5	3	5
performance	1/3	1	3	1	3
Manufacturing method	1/5	1/3	1	1	3
Cost	1/3	1	1	1	3
Availability	1/5	1/3	1/3	1/3	1
Total sum	2.067	5.667	10.333	6.333	15

Step 5. Integrating or synthesizing the pair-wise comparison

To determine the priority vectors, the average normalized column approach is employed (Ariff, Salit et al. 2008). The vector of priority can be calculate mathematically as the follows:

$V_i = \frac{1}{n}\sum_{j=1}^{n}\left(\frac{m_{ij}}{\sum_{i=1}^{n} m_{ij}}\right)$ where $i, j = 1, 2, 3, \ldots n, V_i =$ periorities of vector, and $m =$ each value of column criteria.

$$\sum_{i=1}^{n} m_{ij} = 1 + 0.333 + 0.2 + 0.333 + 0.2 = 2.067$$

$$= 3 + 1 + 0.333 + 1 + 0.333 = 5.667$$

$$= 5 + 3 + 1 + 1 + 0.333 = 10.333$$

$$= 3 + 1 + 1 + 1 + 0.333 = 6.333$$

$$= 5 + 3 + 3 + 3 + 1 = 15$$

$$\frac{m_{ij}}{\sum_{i=1}^{n} m_{ij}} = \frac{1}{2.067} = 0.484, \frac{0.333}{2.067} = 0.161, \frac{0.2}{2.067} = 0.097, \frac{0.333}{2.067} = 0.161, \frac{0.2}{2.067} = 0.097$$

$$= \frac{3}{5.667} = 0.53, \frac{1}{5.667} = 0.176, \frac{0.333}{5.667} = 0.059, \frac{1}{5.667} = 0.176, \frac{0.333}{5.667} = 0.059$$

$$= \frac{5}{10.333} = 0.484, \frac{3}{10.333} = 0.29, \frac{1}{10.333} = 0.097, \frac{1}{10.333} = 0.097, \frac{0.333}{10.333} = 0.032$$

$$= \frac{3}{6.333} = 0.474, \frac{1}{6.333} = 0.158, \frac{1}{6.333} = 0.158, \frac{1}{6.333} = 0.158, \frac{0.333}{6.333} = 0.053$$

$$= \frac{5}{15} = 0.333, \quad \frac{3}{15} = 0.2, \quad \frac{3}{15} = 0.2, \quad \frac{3}{15} = 0.2, \quad \frac{1}{15} = 0.067$$

$$\sum_{j=1}^{n} \left(\frac{m_{ij}}{\sum_{i=1}^{n} m_{ij}} \right) = 0.484 + 0.53 + 0.484 + 0.474 + 0.333 = 2.305$$

$$= 0.161 + 0.176 + 0.29 + 0.158 + 0.2 = 0.985$$

$$= 0.097 + 0.059 + 0.097 + 0.158 + 0.2 = 0.61$$

$$= 0.161 + 0.176 + 0.097 + 0.158 + 0.2 = 0.792$$

$$= 0.097 + 0.059 + 0.032 + 0.053 + 0.067 = 0.31$$

As the result, the sum was divided by the total number of elements ($n = 5$).

$$2.305/5 = 0.46$$

$$0.985/5 = 0.2$$

$$0.61/5 = 0.12$$

$$0.792/5 = 0.158$$

$$0.31/5 = 0.062$$

Table 6: Synthesized matrix for the criteria

Criteria	Energy absorption	Performance	Manufacturing method	Cost	Availability	Total row	Priority vector
Energy absorption	0.484	0.53	0.484	0.474	0.333	2.305	0.46
Performance	0.161	0.176	0.29	0.158	0.2	0.985	0.2
Manufacturing method	0.097	0.059	0.097	0.158	0.2	0.61	0.12
cost	0.161	0.176	0.097	0.158	0.2	0.792	0.158
Availability	0.097	0.059	0.032	0.053	0.067	0.31	0.062
Σ	1.000						

The analysis summation of priority vector weight is one in this case; if the summation of priority vector weight is one, then the problem is in the right way.

Step 6. Decide its consistency (perform consistency)

There can be inconsistency because the value comparisons are personnel subjective. The end consistency operation should verify to ensure that the decisions are consistent. Consistency ratio (C_R) is used to decide the consistency and for same order of matrices is calculated as;

$$C_R = \frac{C_I}{R_I}$$

Where, C_R = Consistency ratio

C_I = Consistency index

R_I = Random index

To calculate C_R, three steps could be applied as follows:

Finding the Eigenvalue (λ_{max}) is the first step and obtained by multiplying the right built matrix of decisions by the priority vector to get a new vector.

$$1 * 0.46 + 3 * 0.2 + 5 * 0.12 + 3 * 0.158 + 5 * 0.062 = 2.444$$

$$1/3 * 0.46 + 1 * 0.2 + 3 * 0.12 + 1 * 0.158 + 3 * 0.062 = 1.06$$

$$1/5 * 0.46 + 1/3 * 0.2 + 1 * 0.12 + 1 * 0.158 + 3 * 0.062 = 0.623$$

$$1/3 * 0.46 + 1 * 0.2 + 1 * 0.12 + 1 * 0.158 + 3 * 0.062 = 0.82$$

$$1/5 * 0.46 + 1/3 * 0.2 + 1/3 * 0.12 + 1/3 * 0.158 + 1 * 0.062 = 0.313$$

Then, By dividing each given weighted sum matrix member by its corresponding priority vector value,

$$2.44/0.46 = 5.313$$

$$1.06/0.2 = 5.3$$

$$0.623/0.12 = 5.19$$

$$0.82/0.158 = 5.19$$

$$0.313/0.062 = 5.05$$

Then, find Eigenvalue (λ_{max}) by analyzing average priority vectors.

$$\lambda_{max} = (5.313 + 5.3 + 5.19 + 5.19 + 5.05)/5 = 5.21$$

Determine the Index of Consistency (C_I),

$$C_I = (\lambda_{max} - n)/(n-1)$$

Where matrix size(n)=5, $C_I = (5.21 - 5)/(5 - 1) = 0.052$

Calculate the Consistency Ratio

By using (Ariff, Salit et al. 2008, Ihimekpen, Isagba et al. 2017) of table 8, Determine the Index of Consistency(RI) for matrix size of 5.

Random Index for a matrix size of 5 = 1.12.

Table 7: AHP random index for different matrices size

Size of matrix (n)	1	2	3	4	5	6	7	8	9	10	11	12
Random index (RI)	0	0	0.58	0.9	1.12	1.24	1.32	1.41	1.45	1.49	1.51	1.58

$$C_R = \frac{C_I}{R_I} = \frac{0.052}{1.12} = 0.046 \; which \; is \; < 0.1$$

Therefore, the assigned judgments are acceptable, as proved by the value of C_R is overcome as less than 0.1 in number.

Step 7. The consistency test for the design concepts

For all design alternatives, the Energy Absorption (EA) is more essential than cost in a pairwise process comparison scale (C). Following the same procedures as done above in design criteria, by giving the appropriate pair-wise scale, we have priority vector of each alternatives.

Table 8: Consistency test of each design concepts

Criteria	Priority vectors of Alternatives					
	M – 1	M - 2	M - 3	M - 4	M - 5	M - 6
Energy absorption	0.46	0.373	0.513	0.465	0.54	0.46
Performance	0.2	0.21	0.19	0.21	0.18	0.2

Manufacturing method	0.12	0.15	0.13	0.138	0.122	0.12
Cost	0.158	0.182	0.123	0.138	0.12	0.158
Availability	0.062	0.097	0.047	0.048	0.046	0.062

Step 8. Developing of overall priority rank

To identify the optimal design concept, the entire priority vector needs to be recalculated when the consistency computation is complete.

Table 9: overall priority vectors for design alternatives and criteria's.

criteria's	Priority vector	Alternatives					
		M - 1	M - 2	M - 3	M - 4	M - 5	M - 6
Energy absorption	0.46	0.46	0.373	0.513	0.465	0.54	0.46
performance	0.2	0.2	0.21	0.19	0.21	0.18	0.2
Manufacturing method	0.12	0.12	0.15	0.13	0.138	0.122	0.12
Cost	0.158	0.158	0.182	0.123	0.138	0.12	0.158
Availability	0.062	0.062	0.097	0.047	0.048	0.046	0.062

The priority vector for the design alternatives multiplied by the priority vector of the criteria gives the overall priority vector. For example, the following is an calculation of how M-1's overall priority is determined:

$$0.46 * 0.46 + 0.2 * 0.2 + 0.12 * 0.12 + 0.158 * 0.158 + 0.062 * 0.062 = 0.295$$

Table 10: over all priority vector of alternatives in relation to the criteria

Alternatives	**Priority vector**					**Overall priority vector**
	Energy absorption (E_A)	Performance (P)	Manufacturing method (M)	Cost (C)	Availability (A)	
	0.46	**0.2**	**0.12**	**0.158**	**0.062**	
M-1	0.46	0.2	0.12	0.158	0.062	0.295
M-2	0.373	0.2	0.15	0.18	0.097	0.264
M-3	0.513	0.19	0.13	0.12	0.047	0.312
M-4	0.465	0.21	0.138	0.138	0.048	0.3
M-5	0.54	0.18	0.122	0.12	0.046	0.33
M-6	0.46	0.2	0.12	0.158	0.062	0.295

.

Step 9 Best design material selection

According to table 11. shows that material 5 (M-5) has the highest value (0.184 or 18.4%) among the other design alternatives that is appropriate for further development. With a score of 0.174 (17.4%), design material 3 (M-3) comes in second place, and design material 2 (M-2) comes in last with a value of just 0.145 (14.5%). Out of the six design concepts, M-5 has the highest value, making it the recommended option.

Table 11: Ranking of materials

	Rank	
1	M-5	0.184 or (18.4%)
2	M-3	0.174 or (17.4%)
3	M-4	0.167 or (16.7%)
4	M-1	0.1643 or (16.3%)
5	M-6	0.164 or (16.4%)
6	M-2	0.145 or (14.5%)

Based on the evaluation criteria, GFRE emerged as the best choice for polymer composite bumper materials. It offers a combination of excellent energy absorption, mechanical performance, cost-effectiveness, and availability that meets the stringent requirements of automotive applications, having the highest value (18.4%).

3.2.3 Description of reinforcement materials

Fibers used in polymer composites include glass, carbon, aramid, natural fibers, and synthetic polymer fibers. Glass, carbon, and aramid fibers are commonly classified as high-performance reinforcement fibers due to their high strength and stiffness. In addition to these, several synthetic polymer fibers such as polyethylene, polypropylene, nylon, and polyester are also used in composite structures. While some polymer fibers may exhibit lower stiffness compared to carbon or glass fibers, many engineered polymer fibers possess excellent specific strength, impact resistance, fatigue performance, and toughness, making them suitable for structural and semi-structural applications.

Glass fiber, is a material made up of many incredibly fine glass fibers; it has mechanical qualities that are roughly comparable to those of other fibers, such as carbon fiber and polymers; it is not as stiff as carbon fiber, but it is significantly less expensive and less brittle when used in composites (El-Wazery, El-Elamy et al. 2017). Corrosion resistance, electrical characteristics, impact resistance, low density, and specific strength are typical properties of glass fiber.

3.2.3.1 Classification of glass fibers

The following benefits make glass fibers the most popular reinforcing material for composites: Melted glass is easily pulled into high-strength fibers, making the composite form of relatively strong fibers simple to produce. The AHP technique shows that S-glass is more resistant to heat, moisture, and chemicals than E glass.

Table 12. The mechanical and physical characteristics of GF (Srivastava, Kumar et al. 2022).

Fiber	Density (g/cm^3)	Tensile Strength (GPa)	Young's modulus (GPa)	Elongation (%)	Coefficient of thermal expansion ($10^{-7}/^oC$)	Poison's ratio
E - Glass	2.58	3.445	72.3	4.8	54	0.2
C - Glass	2.52	3.310	68.9	4.8	63	-
S2- Glass	2.46	4.890	86.9	5.7	16	0.22
A - Glass	2.44	3.310	68.9	4.8	73	-
D - Glass	2.11-2.14	2.415	51.7	4.6	25	-
R - Glass	2.54	4.135	85.5	4.8	33	-
EGR - Glass	2.72	3.445	80.3	4.8	59	-
AR Glass	2.70	3.241	73.1	44	65	-

Table 13. composition (%) of glass fibers (Jay P. S, Pankaj K, 2022).

Type	(SiO_2)	(AI_2O_3)	Tio_2	B_2o_3	(CaO)	(MgO)	Na_2O	K_2O	Fe_2O_3
E-Glass	55.0	14.0	0.2	7.0	22.0	1.0	0.5	0.3	-
C- Glass	64.6	4.1	-	5.0	13.4	3.3	9.6	0.5	-
S- Glass	65.0	25.0	-	-	-	10.0	-	-	-
A- Glass	67.5	3.5	-	1.5	6.5	4.5	13.5	3.0	-
D- Glass	74.0	-	-	22.5	-	-	1.5	2.0	-
R- Glass	60.0	24.0	-	-	9.0	6.0	0.5	0.1	-
EGR-Glass	61.0	13.0	-	-	22.0	3.0	-	0.5	-
Basalt	52.0	17.2	1.0	-	8.6	5.2	5.0	1.0	5.0

S glass fiber

S glass fiber having Magnesium-aluminosilicate, which is primarily utilized as reinforcement in structural applications requiring for great strength and durability at high temperatures. S-glass fibers have better mechanical qualities than carbon and aramid fibers. When improved performance is needed, this high-strength glass fiber is employed. Because these fibers have a lower density than E-glass, the laminate is lighter and more rigid. S-glass is less expensive than aramid or carbon fiber and has better mechanical qualities than E-glass (El-Wazery, El-Elamy et al. 2017). High performance S Glass fiber is available commercial name of S-2 Glass Fiber with roving's, yarns, chopped fibers forms as shown in the figure 17.

Figure 17. Forms of S-2 Glass Fiber (El-Wazery, El-Elamy et al. 2017)

3.2.3.2 Description of matrix materials

By serving as a glue to keep the reinforcing fibers together and protect them from environmental and mechanical effect, the resin's main function is to transfer stress between them. Both thermoplastic and thermoset resins are utilized in reinforced polymer composites (El-Wazery, El-Elamy et al. 2017). Polypropylene, polyurethane, poly-vinyl chloride, acrylonitrile betadine styrene, and epoxy resins are among the various high-performance plastic resin types that are frequently utilized as matrix materials for automobile bumpers.

Epoxy resin: The most often utilized type of resin is epoxy. These organic liquids have a low molecular weight and include epoxide groups. Most often, epichlorohydrin and aromatic amines react to generate epoxides, which have rings with one oxygen atom and two carbon atoms. Epoxy resins are well-known for their ability to repair concrete and a variety of composite parts and structures. A variety of products with differing levels of performance can be produced by engineering the resins' structure. One important advantage of epoxy is its ability to be combined with other epoxy resins or made with other materials to obtain particular performance qualities. Epoxy is mostly used to create high-performance composites with better mechanical qualities,

including resistance to corrosive liquids and conditions, better electrical qualities, and good performance.

Its popularity surpasses that of other polymer matrices, despite the fact that it is more expensive. Due to diversity, availability, good strength, low viscosity, low shrinkage, and good compatibility with glass fibers.

Table 14. Properties of the three most commonly used resin materials.

Properties	**Poly ester**	**Poly-vinyl chloride**	**Epoxy**
Stiffness in GPa	2.4-2.6	2.98-3.4	3.65
Ultimate strength in MPa	41.5-85	52-80	65-85
Ultimate strain in %	1.25-4.5	5.0	5.0-3.0
Density in Kgm^{-3} ***$*10^3$***	(1.15-1.25)	(1.15-1.25)	1.15-1.4
Curing shrinkage in %	6.0-8.0	5.4-7.05	Below 2.0

3.2.3.3 Fiber-reinforced polymer (FRP)

S-glass/epoxy and S2-glass/epoxy composites.

S-glass reinforced epoxy and S2-Glass/Epoxy composites are both high-performance materials composed of strong glass fibers embedded in an epoxy resin matrix. These composites are widely utilized in sectors such as aerospace, automotive, and marine, where enhanced strength, stiffness, and resistance to impact are essential.

1. **Glass fibers**: S-Glass fibers are produced from magnesium-alumino-silicate glass and are recognized for their superior tensile strength, stiffness (modulus), and elongation at break when compared to more conventional fibers like E-Glass. Owing to these mechanical advantages, S-Glass is frequently selected for structural applications requiring elevated mechanical performance. S2-Glass represents an advanced version of S-Glass, offering improved tensile

strength and enhanced resistance to impact. Although the base glass composition remains similar, S2-Glass features finer fiber diameters and better fatigue performance. These characteristics make it particularly well-suited for environments involving extreme mechanical loads and where impact durability is critical.

2. **Epoxy resin**: Both S-glass reinforced epoxy and S2-glass reinforced epoxy composites incorporate epoxy resin as the matrix material. Epoxy is a thermosetting polymer known for curing at elevated temperatures and providing excellent adhesion, chemical resistance, and mechanical strength. The epoxy matrix ensures effective bonding between fibers, contributing to the composite's overall structural integrity and improved material performance over its individual components..

3. **Mechanical properties**: Composites made with S2-Glass fibers typically exhibit better mechanical properties than those using S-Glass. These include higher tensile strength, increased stiffness, and greater resistance to impact. As a result, S2-glass reinforced epoxy composites are more appropriate for applications that involve high mechanical stress or require superior durability and load-bearing capability.

4. **Cost consideration**:- S2-glass reinforced epoxy composites typically come at a higher price point compared to S-glass reinforced epoxy composites, primarily due to the increased cost of producing S2-Glass fibers. Despite the added expense, the superior mechanical characteristics of S2-glass reinforced epoxy, such as enhanced strength, stiffness, and impact resistance can justify the investment, especially in applications where top-tier performance is critical.

5. **Typical application**:- Both types of composites are widely used across industries that demand high performance from materials S-glass reinforced epoxy is often chosen for applications that require solid mechanical capabilities but also demand cost efficiency. Conversely, S2-glass reinforced epoxy is favored for scenarios where maximum strength, fatigue life, and impact resistance are essential, such as in aerospace structures, military equipment, and advanced automotive components.

In summary, S-glass reinforced epoxy and S2-glass reinforced epoxy composites both offer excellent mechanical performance, including high strength and impact resistance. However, S2-glass reinforced epoxy generally surpasses S-glass reinforced epoxy in terms of performance

metrics. This improvement comes with a higher material cost, making the selection between the two largely dependent on the specific performance demands and budget constraints of the application.

Glass/Epoxy Composites in Automotive Applications

S2-glass reinforced epoxy composite for car bumper application

A glass/epoxy composite is a material made by combining glass fibers with an epoxy resin matrix, resulting in a strong, lightweight, and adaptable composite. This type of material is widely used in industries such as automotive, aerospace, and marine due to its favorable balance of mechanical and physical properties. Specifically, for automotive bumpers, glass/epoxy composites especially those reinforced with S2-glass fibers offer several key advantages:

1. **Reduced weight**: Compared to conventional materials like steel, glass/epoxy composites are significantly lighter. This weight reduction contributes to improved vehicle fuel efficiency and performance. Lower mass also means reduced emissions and energy consumption during operation (Abhemanyu, Prassanth et al. 2019).
2. **High strength and stiffness**:- S2-glass reinforced epoxy composites are known for their excellent strength-to-weight and stiffness-to-weight ratios. This ensures that the bumper is capable of withstanding impact forces while maintaining structural integrity and occupant protection.
3. **Durability and Corrosion Resistance**:- One of the notable benefits of glass/epoxy materials is their resistance to environmental degradation, including corrosion, UV exposure, and moisture. Unlike metals, these composites do not rust or weaken due to chemical exposure, which extends the bumper's service life (Dhakal, Zhang et al. 2007).
4. **Design Versatility**:- Glass/epoxy composites can be easily shaped into complex geometries that are difficult to produce with metals. This design flexibility enables automotive engineers to create bumpers that are both functional and aesthetically optimized.
5. **Superior Energy Absorption**:- Thanks to their high impact resistance, glass/epoxy composites can absorb significant amounts of kinetic energy during collisions. This energy dissipation capacity reduces the force transmitted to the vehicle's occupants, potentially lowering the risk of injury.

3.2.3.4 Properties of S-glass reinforced epoxy and S2-glass reinforced epoxy composites

According to (www.agy.com) the elastic and strength properties of S2-glass reinforced epoxy Composites make them highly suitable for use in impact-critical applications such as those found in the automotive, aerospace, and defense industries. The data at the maximum, for the design of automobile structures, takes the form of those shown in Table 15.

Table 15. Typical properties.S-2 Glass Fiber Unidirectional Epoxy Composite.

PROPERTIES	**ASTM STANDARD**	**UNIT (AT 22^{O}C)**
Elastic Constants		Gpa
Longitudinal Modulus	D3039	53-59
Transverse Modulus	D3039	16-20
Axial Shear Modulus	D3518	6-9
Poission's Ratio	D3039	0.26-0.28
Strength Properties		Mpa
Longitudinal Tension	D3039	1540-2000
Longitudinal Compression	D3410	690-1240
Transverse Tension	D3039	41-82
Transverse Compression	D3410	110-200
In Plane Shear	D3518	62-165
Interlaminar Shear	D2344	155-103
Ultimate Strains		%
Longitudinal Tension	D3039	2.7-3.5

Longitudinal Compression	D3410	1.1-1.8
Transverse Tension	D3039	0.25-0.5
Transverse Compression	D3410	1.1-2
In Plane Shear	D3518	1.6-2.5
Physical Properties		
Fiber Volume	D2734	57-63%
Density	D792	1.96-2.5 G/Cm^3

3.2.3.4.1 Comparison on typical properties of S-Glass fiber/epoxy and S2-Glass fiber/epoxy composites

S2-glass reinforced epoxy and S-glass reinforced epoxy unidirectional composites with a 0.6 fiber fraction have different properties due to their distinct fiber and epoxy types. S2-glass fibers have superior characteristics in terms of tensile strength, impact resistance, and stiffness compared to S-glass fibers. These differences in fiber properties affect the overall mechanical performance of the composites.

1. **Elastic constants (in GPa):** S2-glass reinforced epoxy: The elastic modulus of S2-glass reinforced epoxy composite ranges from 45 to 59 GPa (da Silva, de Araújo Silva et al. 2022).

S-glass reinforced epoxy: The elastic modulus of S-glass reinforced epoxy composite ranges from 35 to 45 GPa (El-Wazery, El-Elamy et al. 2017).

The S2-glass reinforced epoxy composite has a higher elastic modulus, approximately 22% to 57% higher than that of the S2-glass reinforced epoxy composite.

2. **Strength properties (in MPa):** S2-glass reinforced epoxy: The tensile strength of S2-glass reinforced epoxy composite ranges from 1100 to 1300 MPa (Abd-Ali and Madeh 2016).

S-glass reinforced epoxy: The tensile strength of S-glass reinforced epoxy composite ranges from 900 to 1100 MPa (Sonawane and Shelar 2018).

The S2-glass reinforced epoxy composite has a higher tensile strength, approximately 18% to 44% higher than that of the S-glass reinforced epoxy composite.

3. **Ultimate strains (in %):** S2-glass reinforced epoxy: The ultimate strain for S2-glass reinforced epoxy composite ranges from 2.5% to 3.5% (Olorunnishola and Adubi 2018, da Silva, de Araújo Silva et al. 2022).

S-glass reinforced epoxy: The ultimate strain for S-glass/epoxy composite ranges from 2.0% to 3.0% (El-Wazery, El-Elamy et al. 2017, da Silva, de Araújo Silva et al. 2022).

The S2-glass/epoxy composite has a higher ultimate strain, approximately 25% to 50% higher than that of the S-glass epoxy composite.

Overall, S2-glass reinforced epoxy composites have superior mechanical properties compared to S-glass reinforced epoxy composites due to their improved fiber and epoxy characteristics. For automobile bumper applications, the combination of a resin transfer molding process and continuous fiber alignment can enhance the properties of both composites. The higher stiffness, strength, and strain capacities of the S2-glass reinforced epoxy composite make it a more suitable candidate for automotive bumper applications, ensuring better protection and impact resistance.

3.2.3.4.2 Selection of fiber alignment, resin type, and fabrication methods for S2-glass reinforced epoxy composites

For S2-glass reinforced epoxy unidirectional composite with a fiber volume fraction of 0.6, used in automotive bumper systems, the following parameters contribute to achieving superior mechanical performance:

1. Fiber Alignment: Fibers should be aligned in the direction of primary impact or load-bearing (typically longitudinal), ensuring maximum tensile and flexural strength in critical areas (Chawla 2012).

2. Resin Type: The use of an epoxy resin is already mentioned in the question. High-performance **epoxy resin** is preferred widely used matrix material in high-performance composite applications due to their superior mechanical properties, chemical resistance, and adhesion to reinforcement fibers (Gupta et al., 2017).

3. Fabrication Method: Resin Transfer Molding (RTM) or Vacuum-Assisted Resin Transfer Molding (VARTM) can be used for fabricating complex-shaped parts with good mechanical properties (Fong and Advani 1998). These processes can result in a better wet-out (impregnation) of the fibers, ensuring a uniform fiber fraction throughout the composite.

The exact numerical values of mechanical properties depend on the specific materials and process employed. For example, the tensile strength of S2-glass fibers can range from 1700 - 2100 MPa, while the tensile strength of typical epoxy resins can vary between 60 - 80 MPa (Chawla 2012).

3.2.4 Theoretical UD lamina analysis

The majority of composite materials are created by stacking many separate layers of ply or unidirectional lamina. The matrix and fiber used to make each lamina are identical. A unidirectional lamina with corresponding longitudinal and transverse orientations is shown in the figure 18.

How stiff the lamina and laminate are determined by;

- Fiber and matrix volume fraction
- Reinforcement used
- Fiber orientation

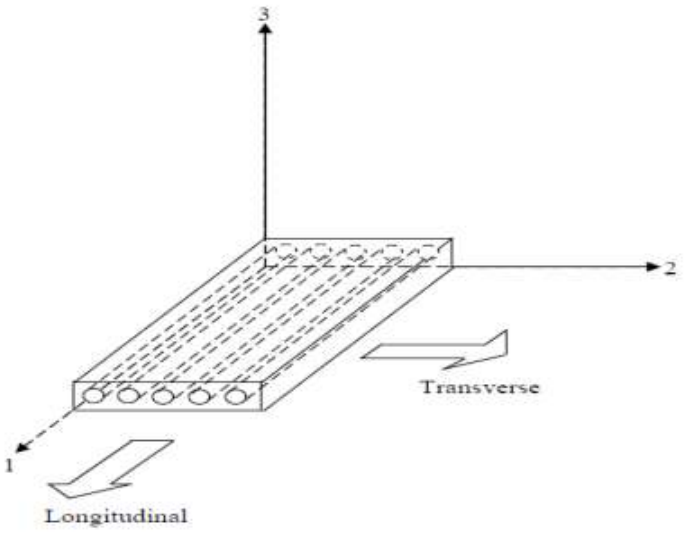

Figure 18. UD composite lamina composite lamina

The Halpin/Tsai model and the rule of mixture are the two theoretical models that are used to compute the ply or unidirectional lamina characteristics.

Rule of mixture

Bulk properties(Young's and Shear moduli) of the raw material and basic properties of composite materials that can be approximated based on the contribution of each portion of the composite, can be used to characterize the deformation of homogeneous, isotropic materials in a reasonably straightforward manner. This technique is called law of mixing.

For a two component composite;

$$V_f + V_m = 1 \text{.....} Eq\ 1$$

Where, V_f = fiber Volume fraction

V_m = matrix Volume fraction

Based on the rule of mixture axial load applied along longitudinal direction (P_c) can be calculated by;

$$P_c = P_f V_f + P_m V_m \text{.....} Eq\ 2$$

$$P_c = P_f V_f + P_m (1 - V_f) \text{.....} Eq\ 3$$

Where, P_c= axial load is applied in the longitudinal direction

Shear modulus of the fiber and matrix resin can be calculated by:

$G = \frac{E}{2(1+v)}$.....Eq 4

Where E is elastic modulus and v is Poisson's ratio of the fiber or matrix resin.

longitudinal elastic modulus can be calculated based on rule of mixing;

$E_{1y} = V_f E_{1f} + E_m (1 - V_f) = E_{11}$.....Eq 5

Where, E_{1f} and E_m are longitudinal elastic modulus the fiber and matrix respectively.

The mixture ratio formula provides accurate longitudinal elastic modulus estimation, however it performs poorly in transverse directions. Therefore, the transverse modulus and shear modulus are calculated using the Halpin–Tsai equations.

$$E_2^y = \frac{(1+\xi\eta V_f)}{1-\eta V_f} \text{.....Eq 6}$$

$$\eta = \frac{E_{2f}/E_m - 1}{E_{2f}/E_m - \xi} \text{.....} Eq\ 7$$

Where E_2^y is the fibers elastic modulus in transverse direction.

ξ, a measure of fiber reinforcement depends on the fiber geometry, packing manner, and loading type. For calculating typical properties, it has been shown that ξ = 1 produces more accurate results but For fibers with a circular section, ξ = 2 is recommended. Therefore, using ξ = 1 yields the shear modulus.

$$G_{12y} = G_m \frac{(G_{12f}+G_m)+V_f(G_{12f}-G_m)}{(G_{12f}+G_m)-V_f(G_{12f}-G_m)} \text{.....} Eq\ 8$$

Where G_m and G_{12f} the shear modulus of the matrix and fiber respectively.

Poisson's ratios of the fiber and matrix, as well as the fiber's volume ratio, can be used to determine the major Poisson's ratio of resin-immersed fiber. An inverse relationship with the elastic moduli can be used to find the minor Poisson's ratio.

$$V_{12}^y = V_f V_{12f} + V_m(1 - V_f) \text{.....} Eq\ 9$$

Where, $V_{12f}$and V_m are the fiber and matrix poison's ratio respectively.

$$V_{21}^y = V_{12}^y \frac{E_2^y}{E_1^y} \text{.....} Eq\ 10$$

The longitudinal and transverse elastic moduli and poison's ratio can be calculated by using the rule of mixtures approach:

$$E_1 = E_2 = 0.5(E_1^y + E_2^y) \text{.....Eq 11}$$

$$V_{12} = V_{21} = 0.5(V_{12}^y + V_{21}^y) \text{.....Eq 12}$$

$$G_{23} = \frac{E_2}{2(1+V_{12})} \text{.....Eq 13}$$

$$v_{23} = v_f V_f + v_m(1 - v_f) \left[\frac{1+v_m - v_{12}\frac{E_m}{E_1}}{1-v_m^2+v_m v_{12}\frac{E_m}{E_1}}\right] \text{..... Eq 14}$$

Composite elongation is the sum of the elongation of matrix and fiber

$$\delta_c = \delta_m + \delta_f \text{.....Eq 15}$$

Halpin/Tsai model. In order to determine the longitudinal, transverse, and shear moduli of composite materials, a generalized semi-empirical formula has been applied. This formula approximates the modulus of composite materials whose fiber volume percentage is less than 1 (Halpin 1969).

$$E_{11} = E_m \frac{(1+\xi_{11}\eta_{11}V_f)}{(1-\eta_{11}V_f)} \text{.....Eq 17}$$

$$E_{22} = E_m \frac{(1+\xi_{22}\eta_{22}V_f)}{(1-\eta_{22}V_f)} \text{.....Eq 18}$$

$$G_{12} = G_m \frac{(1+\xi_{12}\eta_{12}V_f)}{(1-\eta_{12}V_f)} \text{.....Eq 19}$$

$$\xi_{12} = (wt)^{1.73} + 40(V_f)^{10} \text{.....Eq 20}$$

$$\xi_{11} = 2(1t) + 40(V_f)^{10} \text{.....Eq 21}$$

$$\xi_{22} = 2(wt) + 40(V_f)^{1} \text{.....Eq 22}$$

$$\eta_{11} = \frac{(\frac{E_f}{E_M}-1)}{(\frac{E_f}{E_M}+\xi_{11})} \text{.....Eq 23}$$

$$\eta_{22} = \frac{(\frac{E_f}{E_M} - 1)}{(\frac{E_f}{E_M} + \xi_{22})} \text{.....Eq 24}$$

$$\eta_{12} = \frac{(\frac{G_f}{G_M} - 1)}{(\frac{G_f}{G_M} + \xi_{12})} \text{.....Eq 25}$$

3.2.5 Laminate analysis

The major fiber direction, in-plane direction perpendicular to the fibers, and out-of-plane direction perpendicular to the fibers shall be denoted by the subscripts 1, 2, and 3 for the sake of this study. The primary axes of the orthotropic material behavior are also represented by these numbers.

3D Material Model

For three dimensional stress strain relations for a linear elastic In three dimensions, the strain-stress relations for a typical linear elastic orthotropic material implemented within ANSYS are written as:

$$\{\varepsilon\} = \begin{Bmatrix} \varepsilon_{11} \\ \varepsilon_{22} \\ \varepsilon_{33} \\ \gamma_{12} \\ \gamma_{13} \\ \gamma_{23} \end{Bmatrix} = \begin{bmatrix} s_{11} & s_{12} & s_{13} & 0 & 0 & 0 \\ s_{21} & s_{22} & s_{23} & 0 & 0 & 0 \\ s_{31} & s_{32} & s_{33} & 0 & 0 & 0 \\ 0 & 0 & 0 & s_{44} & 0 & 0 \\ 0 & 0 & 0 & 0 & s_{55} & 0 \\ 0 & 0 & 0 & 0 & 0 & s_{66} \end{bmatrix} \begin{Bmatrix} \sigma_{11} \\ \sigma_{22} \\ \sigma_{33} \\ \sigma_{12} \\ \sigma_{13} \\ \sigma_{23} \end{Bmatrix} = [s]\{\sigma\} \text{.....Eq 26}$$

Hence the shear components are totally uncoupled, it is shows that the normal components are coupled to one another. The elastic engineering material constants are used to define the compliance coefficients Sij in the matrix provided in Eq. 26.

$$S_{11} = \frac{1}{E_{11}}; S_{22} = \frac{1}{E_{22}}; S_{33} = \frac{1}{E_{33}}; \text{.....Eq 27}$$

$$S_{12} = S_{21} = -\frac{V_{21}}{E_{22}} = -\frac{V_{12}}{E_{11}} \text{.....Eq 28}$$

$$S_{13} = S_{31} = -\frac{V_{23}}{E_{33}} = -\frac{V_{12}}{E_{11}} \text{.....} Eq\ 29$$

$$S_{23} = S_{32} = -\frac{V_{32}}{E_{33}} = -\frac{V_{23}}{E_{22}} \text{.....} Eq\ 30$$

$$S_{44} = \frac{1}{G_{12}}; S = \frac{1}{G_{13}}; S = \frac{1}{G_{23}}; \text{.....} Eq\ 31$$

The stress strain relations ca be calculated from the compliance relations Eq 27-31 as;

$$\{\sigma\} = \begin{Bmatrix} \sigma_{11} \\ \sigma_{22} \\ \sigma_{33} \\ \sigma_{12} \\ \sigma_{13} \\ \sigma_{23} \end{Bmatrix} = \begin{bmatrix} C_{11} & C_{12} & C_{13} & 0 & 0 & 0 \\ C_{21} & C_{22} & C_{23} & 0 & 0 & 0 \\ C_{31} & C_{32} & C_{33} & 0 & 0 & 0 \\ 0 & 0 & 0 & C_{44} & 0 & 0 \\ 0 & 0 & 0 & 0 & C_{55} & 0 \\ 0 & 0 & 0 & 0 & 0 & C_{66} \end{bmatrix} \begin{Bmatrix} \varepsilon_{11} \\ \varepsilon_{22} \\ \varepsilon_{33} \\ \gamma_{12} \\ \gamma_{13} \\ \gamma_{23} \end{Bmatrix} = [S]^{-1}\{\varepsilon\} = [C]\{\varepsilon\} \text{.....} Eq\ 32$$

The elastic material constants in the matrix above are used to define the stiffness coefficients C_{ij}.

$$C_{11} = \frac{(1-V_{23}V_{32})E_{11}}{\Delta}; C_{22} = \frac{(1-V_{13}V_{13})E_{22}}{\Delta}; C_{33} = \frac{(1-V_{12}V_{21})E_{33}}{\Delta}; \text{.....} Eq\ 33$$

$$C_{12} = C_{21} = \frac{(V_{12}+V_{13}V_{32})E_{22}}{\Delta} = \frac{(V_{21}+V_{31}V_{23})E_{11}}{\Delta}; \text{.....} Eq\ 34$$

$$C_{13} = C_{31} = \frac{(V_{13}+V_{12}V_{32})E_{33}}{\Delta} = \frac{(V_{31}+V_{21}V_{23})E_{11}}{\Delta}; \text{.....} Eq\ 35$$

$$C_{23} = C_{32} = \frac{(V_{23}+V_{13}V_{21})E_{33}}{\Delta} = \frac{(V_{32}+V_{31}V_{12})E_{22}}{\Delta}; \text{.....} Eq\ 36$$

$$C_{44} = G_{12}; C_{55} = G_{13};\ C_{66} = G_{23}$$

$\Delta = 1 - V_{12}\ V_{21} - V_{23}V_{32} - 2\ V_{21}V_{32}\ V_{13}$.

For three-dimensional elasticity, the reciprocity relations are;

$$E_{11}V_{21} = E_{22}V_{12}$$

$$E_{11}V_{31} = E_{33}V_{13}$$

$$E_{22}V_{32} = E_{33}V_{23}$$

By reducing the compliance matrix in Eq 2 to 2-D behavior he stress components σ33, τ13, and τ23 becomes zero. are obtained by reducing the compliance matrix in Eq 24 to 2-D behavior (sheet analysis).

If the compliance matrix in Eq 26 is reduced to 2-D behavior, the stress components σ33 = τ13 = τ23 = 0. The third, fifth, and sixth rows and columns are removed, and yielding Eq 34.

$$\begin{Bmatrix}\varepsilon_{11}\\ \varepsilon_{22}\\ \sigma_{12}\end{Bmatrix}=\begin{bmatrix}\frac{1}{E1} & -\frac{V21}{E2} & 0\\ -\frac{V12}{E1} & \frac{1}{E2} & 0\\ 0 & 0 & \frac{1}{G12}\end{bmatrix}\begin{Bmatrix}\sigma_{12}\\ \sigma_{22}\\ \gamma_{12}\end{Bmatrix}\text{.....Eq 37}$$

By inverting the 2-D compliance matrix it gives the 2-D stiffness matrix.

.

$$\begin{Bmatrix}\sigma 11\\ \sigma 22\\ \varepsilon 12\end{Bmatrix}=\begin{bmatrix}\frac{E1}{1-V12V21} & \frac{V12E2}{1-V12V21} & 0\\ \frac{V21E1}{1-V12V21} & \frac{E2}{1-V12V21} & 0\\ 0 & 0 & G12\end{bmatrix}\begin{Bmatrix}\varepsilon 11\\ \varepsilon 22\\ \gamma 12\end{Bmatrix}\text{.....Eq 38}$$

3.2.6 S2-glass reinforced epoxy UD composite data for ANSYS Workbench

The maximal strength and stiffness of a single fiber or tow or thin unidirectional laminated composite is reflected in the composite data, which are average values produced by the fiber manufacturers from a series of tests as shown in Table 16. These values can be utilized as engineering data in ANSYS Workbench for S2-glass reinforced epoxy unidirectional composite automobile bumper applications.

Table 16. S-2 Glass Fiber Unidirectional Epoxy Composite Properties used as input data for Ansys workbench (Daniel, Ishai et al. 1994).

MATERIAL: S2 GLASS FIBER REINFORCED EPOXY COMPOSITE DENSITY: 1.99g/cm3 RESIN DENSITY:1.2g/cm3 FIBER DENSITY: 2.46g/cm3			RESIN CONTENT(V_m): 40% FIBER CONTENT(V_f): 60%
Elastic properties	**Results**	**Units**	**Remark**
Elastic modulus in fiber direction, E1	*56*	*GPa*	*Property data test*
Transverse elastic modulus in fiber direction, E2	*18*	*GPa*	*Property data test*
Elastic modulus through in thickness in fiber direction, E3	*18*	*GPa*	*Transverse isotropy: $E_{3=}E_2$*
Shear modulus in the 1-2 plane, G_{12}	*7.5*	*GPa*	*Property data test*
Shear modulus in the 2-3 plane, G_{23}	*1.252*	*GPa*	*Based on Eq 13 .*
Shear modulus in the 1-3 plane,G_{13}	*7.5*	*GPa*	*Transverse isotropy: $G_{13=}G_{12}$*
Poisson's ratio in 1-3 plane, ν_{12}	*0.27*		*Property data test*
Poisson's ratio in 2-3 plane, ν_{23}	*0.256*		*Based on Eq 14.*
Poisson's ratio in 1-3 plane, ν_{13}	*0.27*	*GPa*	*Transverse isotropy: $\nu_{13=}\nu_{12}$*
Strength properties	**Results**	**Units**	**Remark**
Tensile strength in the fiber direction, σ_1	*1770*	*MPa*	*Property data test*
Compressive strength in the fiber Direction, $-\sigma_1$	*-965*	*MPa*	*Property data test*
Tensile strength transverse to the Fiber, σ_2	*61.5*	*MPa*	*Property data test*
Compressive strength transverse to the fiber, $-\sigma_2$	*-155*	*MPa*	*Property data test*
Tensile strength through-the-thickness, σ_3	*61.5*	*MPa*	*$\sigma_{3=}\sigma_2$*
Compressive strength through-the thickness, $-\sigma_3$	*-155*	*MPa*	*$-\sigma_{3=}-\sigma_2$*
Shear strength in the 1-2 plane (in plane), τ_{12}	*113.5*	*MPa*	*Property data test*
Shear strength in the 2-3 plane (interlaminar), τ_{23}	*129*	*MPa*	*Property data test*
Shear strength in the 1-3 plane (interlaminar), τ_{13}	*129*	*MPa*	*$\tau23 = \tau13$*
Ultimate strains	***Results***	***Units***	***Remark***
Longitudinal tension	*3.1*	*%*	*Property data test*
Longitudinal compression	*-1.45*	*%*	*Property data test*
Transverse tension	*0.375*	*%*	*Property data test*
Transvers compression	*-1.05*	*%*	*Property data test*
In-plane shear	*2.05*	*%*	*Property data test*
Physical properties	***Results***	***Units***	
Density	*1.99*	*g/cm3*	

3.3 Analysis of the S2-Glass Fiber Reinforced Polymer Composite Based Front Bumper

3.3.1 Mathematical Modeling

The quantity of energy dissipated or absorbed, beam deflection, von Misses stress failure criteria will all be determined in this study using two ways. The first approach is impact mechanics, which states about the conservation of energy.

Impact mechanics. The geometry, stiffness, mass distributions, contact areas, and impact angles of impacted systems in engineering practice are complex and cannot be analyzed or designed using conventional impact dynamics techniques. Therefore, solving engineering problems will be helped by applying the knowledge of the traditional approach in finite element analysis. Conventional methods include:

Stereo mechanics. This approach uses the impulse-momentum law along with conservation of momentum and energy laws. The technique makes advantage of the coefficient of restitution (COR), which is useful to measure the energy variation, for collisions in which energy is lost.

$$COR = \frac{(V_{B0} - V_{A0})}{(V_A - V_B)} \quad \text{.....Eq 39}$$

Where V_{B0} and V_{A0} final velocity of the barrier and vehicle which are zero.

The An elastic collision is characterized by a coefficient of restitution (COR) of 1.0, indicating that no kinetic energy is lost during the impact. In contrast, a COR value of 0 signifies a perfectly plastic collision, where all kinetic energy is absorbed and converted into other forms, such as internal energy. The COR is a useful parameter for estimating how much kinetic energy remains after a collision higher COR values imply that a larger portion of the initial kinetic energy is retained, while lower values indicate that most of it is dissipated or transformed.

In the context of this study, the collision between the front bumper system and the impactor is considered a plastic impact, as indicated by a COR of zero. This type of impact involves complex

behaviors that require transient and nonlinear analysis techniques to model accurately. The impact behavior of the contact region is of particular significance in this analysis.

Energy-Based Approach

This method relies on the principle of conservation of mechanical energy. The energy initially present in the striker originating from its kinetic and potential energy is transferred to the target structure during impact and is stored as strain energy. Maximum stress and deformation in the target occur when the striker's velocity reduces to zero and its energy has been fully absorbed by the system.

Throughout the impact event, total energy remains conserved. Additionally, momentum is conserved before and after the collision. This is because during the brief duration of contact, the internal forces generated between the colliding bodies are significantly greater than any external forces, making the conservation of momentum a valid assumption.

The following is an expression for the energy and momentum conservation equations after the separation point:

$$\frac{1}{2}M_A V_A^2 = \frac{1}{2}K_{eq}\delta_{max.}^2 + \frac{1}{2}M_A V_{A0}^2 + \frac{1}{2}M_B V_{B0}^2 \text{.....Eq 40}$$

Where;

M_A and M_B are the car's and barriers mass, V_A is the vehicle's velocity prior to impact, and V_{B0} and VA0 are the barrier's and the vehicle's final velocities.

Keq is a bumper's equivalent impact stiffness, which is determined by beam analysis's relationship between displacement and response forces.

A principle of momentum conservation before and after impact can be stated as follows at the point of maximal deflection.

$$M_A V_A = (M_A + M_B)V_0 \text{.....} Eq\ 41$$

Maximum deflection is achieved by merging the two equations, specifically equations 40 and 41.

$$\delta_{max.}^2 = \frac{1}{K_{eq}} \frac{M_A M_B}{M_A + M_B} V_B^2 \text{.....} Eq\ 42$$

Equations for energy and momentum conservation after the separation point can be written as follows:

$$\frac{1}{2} M_A V_A^2 = \frac{1}{2} \frac{M_A M_B}{M_A + M_B} V_A^2 + \frac{1}{2} M_A V_{A0}^2 + \frac{1}{2} M_B V_{B0}^2 \text{.....} Eq\ 43$$

$$KE = \frac{1}{2} M_A V_A^2 = \frac{1}{2} \frac{M_A M_B}{M_A + M_B} V_A^2 + \frac{1}{2} M_A V_{A0}^2 + \frac{1}{2} M_B V_{B0}^2 \text{.....} Eq\ 44$$

The linear momentum conservation principle is satisfied in the elasto-plastic impact because the impact forces are equal and opposite.

$$M_A V_A + M_B V_B = M_A V_{A2} + M_B V_{B2} \text{.....} Eq\ 45$$

The Plastic Strain

The kinetic energy of the barrier before the impact is subtracted from the kinetic energy of the vehicle and barrier after the impact to obtain plastic energy ($E_{Plastic}$).

$$E_{Plastic} = \frac{1}{2} M_A V_A^2 + \frac{1}{2} M_B V_B^2 - \frac{1}{2} M_{A2} V_{A2}^2 - \frac{1}{2} M_{B2} V_{B2}^2 \text{.....} Eq\ 46$$

Impact bending.

Impact bending is another method for determining the deflection and stress value.

Von-mises stress theory and failure criteria.

The Von Mises yield criterion, also known as the maximum distortion energy theory, is widely used to predict the onset of yielding or failure in ductile materials under complex loading conditions. It is based on the observation that a material's ability to withstand stress depends not only on the magnitude of the stress, but also on the type and combination of stresses acting on it.

It has been noted that a solid can tolerate extremely high stress when subjected to hydrostatic external pressure. The amount of stress that can be applied is restricted when energy of deformation is to be stored, as in the tensile test.

Total Strain Energy (U)

The total strain energy can be expressed as follows,

$$U = \frac{\sigma\varepsilon}{2} = \frac{F\delta}{2} \text{.....Eq 47}$$

Where U is strain energy, σ is stress, ε is strain and δ is deformation.

This is valid when we assume that the stress-strain curve is roughly linear up to the yield point:

Extending this for three-dimensional case;

$$U = \frac{1}{2}[\sigma_1\varepsilon_1 + \sigma_2\varepsilon_2 + \sigma_3\varepsilon_3] \text{.....Eq 48}$$

Where, σ_1, σ_2, σ_3 and ε_1, ε_2, ε_3 are principal stress and strains respectively.

According to distortion energy, failure by yielding under a combination of stress occurs when the energy of distortion equals or exceeds the energy of distortion measured during the tensile test at yield strength.

According to failure theory:

$$S_y = \frac{1}{2}[\sigma_1^2 + \sigma_2^2 + \sigma_3^2 - (\sigma_1\varepsilon_1 + \sigma_2\varepsilon_2 + \sigma_3\varepsilon_3)]^{1/2} \text{.....Eq 49}$$

The uniaxial tensile stress that would create the same deformation energy as the actual combination of applied stresses is known as the von-mises effective stress or equivalent stress (σe).

$$S_y = \frac{1}{2}\left[\sigma_{xx}^2 + \sigma_{yy}^2 - \sigma_{xx}\sigma_{yy} + 3\tau_{xy}^2\right]^{1/2} \text{.....Eq 50}$$

A **Factor of Safety (FoS)** was applied because composite materials exhibit predictable elastic behavior and the material properties were obtained from certified manufacturer data. Manufacturing variability is assumed to be minimal, and the simulation already includes

conservative assumptions such as a rigid barrier and full energy transfer. Additionally, automotive lightweight design prioritizes weight reduction, so using a larger FoS (e.g., 2.0–3.0) would lead to unnecessary overdesign and increased mass.

The factor of safety is defined as;

$$Safety\ of\ factor \quad = \sigma e / Sy \text{.....Eq 51}$$

Estimation of impact load. The amount of energy transferred (kinetic energy) during the impact was calculated by combing equations (37) and (39);

$$KE = \frac{1}{2}([\frac{M_A M_B}{M_A + M_B}]V_A^2 + M_A V_{A0}^2 + M_B V_{B0}^2) \text{ .....Eq 52}$$

Basic assumptions that we should considered during defining the energy are;

A. Effective mass of the impactor is equal with the tested vehicle ($\mathbf{M_B=M_A}$).
B. Assume the car was carrying one person weighing 70 kg.
C. The barrier is at rest and on rigid level ($\mathbf{V_B=0}$)
D. When all of the striker's energy has been transferred to the bumper, the striker's velocity drops to zero, and maximum deflections and stresses will be achieved ($V_{A0}=V_{B0}=0$).
E. The three different speeds of the vehicle ($\mathbf{V_A}$) for the impact are:
    - **40 km/h:-** Represents low-speed urban collision conditions (city driving limits in many countries range 30–50 km/h). Frequently used in bumper regulation and insurance crash testing.
    - **70 km/h:-** Represents suburban/highway entry collision conditions.
    - **100 km/h** :- Represents severe highway crash conditions.

F. crash time (**T**):-Crash durations in automotive frontal impacts typically range between 0.08 s to 0.15 s (low-to-moderate speed collisions)

    A value of 0.1 s was selected because:
    - It lies within experimentally observed crash pulse durations.
    - It represents a conservative average value.
    - It simplifies force estimation while remaining realistic.

Based on the above assumptions equation (49) is reduced to;

$$KE = \frac{1}{4}[M]V_A^2 \text{.....} Eq\ 53$$

The impact force (F) was calculated as;

$$F = \frac{KE}{T} \text{.....} Eq\ 54$$

It should use the design Factor of Safety, which was determined to be 1.1, Thus, a Factor of Safety (FoS) of 1.1 accounts for minor uncertainties in impact time, small variations in material properties, and approximations introduced during numerical modeling.

$$F_{FSD} = F \times FSD \text{.....} Eq\ 55$$

To perform an area-wise deformation test for the bumper system, the force should be expressed as pressure.

$$P = \frac{F_{FSD}}{A} \text{.....} Eq\ 56$$

Where A is Area of the front face of bumper parts.

Input data

- Mass of the vehicle ($\mathbf{M_A}$) =1740 Kg
- Maximum loads = 70 Kg
- Total mass (**M**)= 1810 Kg
- Front area of the cover, beam, and assembled system part was 0.8407 m^2, 0.18 m^2, and 1.02704 m^2 respectively.

Effective impact mass

The effective impact mass is the portion of the vehicle mass that is dynamically involved in the collision and transfers kinetic energy to the bumper system during impact. It is not the entire vehicle mass, but the equivalent mass concentrated at the impact location representing the inertia of the vehicle components that participate in the crash event.

Material Behavior Assumption

- Composite material is assumed **linearly elastic orthotropic** up to failure.
- Perfect bonding between fiber and matrix.
- No initial defects (voids, delamination, or cracks).
- No strain-rate sensitivity considered.

Table 17. Numerical result of the impact loads

VEHICLE SPEEDS (m/s)	F_{FSD} *(KN)*	*PRESSURE ON COVER (MPA)*	*PRESSURE ON BEAM (MPA)*	*PRESSURE ON ASSEMBLED (MPA)*
11.1	613.27	0.729	3.4	0.59
19.4	1,873.33	2.28	10.4	1.8
27.7	3819.18	4.5	21.2	3.71

The above numerical value, which described in the table 17, shows that the calculated applied pressure at front bumper parts area with different vehicle speed. According to the numerical value as vehicle speed increase the applied pressure also increase.

3.3.2 Geometry modeling

Modeling of bumper beam of the front car.

To be able to develop the Toyota corolla front bumper in a proper way, I have used the collected information regarding the bumper beams of different light-weight cars. The benchmarking was carried out by finding information on internet papers and publications.

The profile of the existing beam is shown in Figure 19, and the hollow beam was made up of metals (such as steel or aluminum). The front construction of the beams is made as light as possible. The process of creating a rounded beam involves placing it under a press that delivers a load on the beam. As the beam is bent outward, the rounded shape improves rigidity.

Table 18. General benchmarking specification (Goez and Rexhepi 2018)

59 different light weight cars		Weight [Kg]	Width [mm]	Length [mm]	Height [mm]	Thickness [mm]
Bumper beam	Max-min	0.83-5.31	4-245.1	435-1421	14-226.9	1.06-4.08
	Ave	2.98	91.58	640.18	122.25	1.85

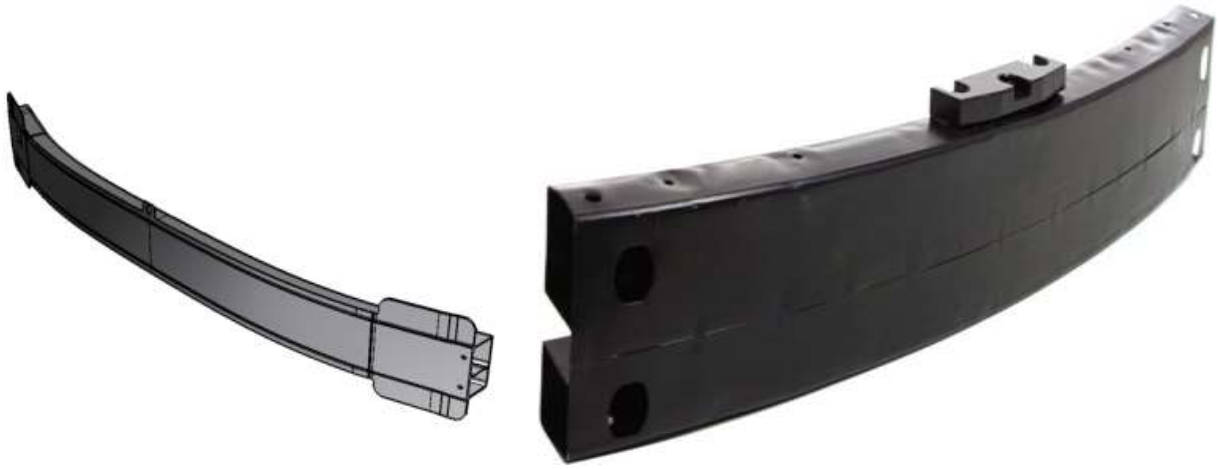

Figure 19. The actual bumper beam profiles of TOYOTA COROLLA SEDAN (2009-2013) model.

A solid model is preferable than a surface model because it gives a more comprehensive picture of an object. In addition to the geometrical information, it offers additional topological information that aids in the clear representation of the solid. Modeling car front bumper beam as shown in Figure 19, was done with help of SOLID WORK and exported as ANSYS step file. The stacked square tubular polymer composite bumpers have a significant improvements in terms of energy absorption(progressive failure), weight, and controlled deformation(plastically deform) than the conventional solid bumper beams. Increasing the radial length and decreasing radius of curvature enhances the flexural modulus, flexural strength, and overall stiffness of the bumper beams during the high velocity impacts (Dhakal, Zhang et al. 2007).

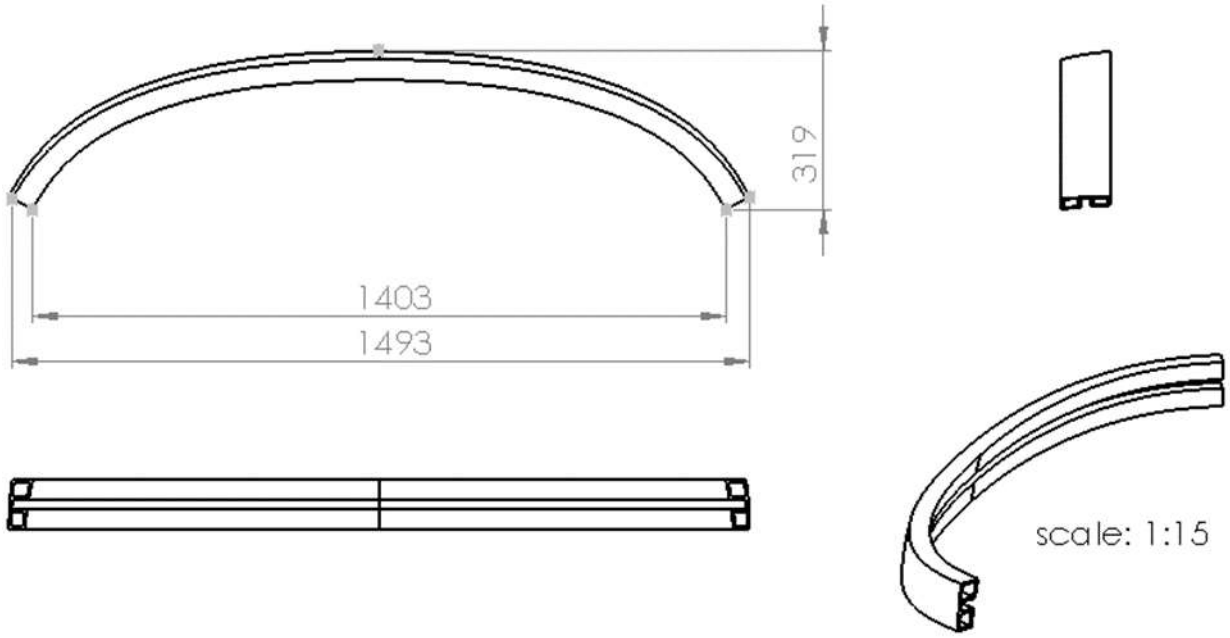

Figure 20. *2*D modelling of the *front car bumper beam*

Modeling of bumper cover. The design and dimension for automobile bumper cover (figure 23) was provided by Autopeflex as shown in the table 19.

Table 19. Dimensions and properties of existing bumper cover.

Parameters	**Values**
Length	*170cm*
Height	*53cm*

Thickness	*0.57cm*
Width	*57cm*
Weight	*8-9.2Kg/set*

Figure 21. The actual bumper cover profiles of TOYOTA COROLLA SEDAN (2009-2013) model.

Modeling of front car bumper cover as shown in Figure 22 and the support in figure 24 was done with help of SOLID WOKRK and exported as ANSYS step file. The support heads was integrated with polymer composite plates, these plates significantly improved the energy absorption capability of the system.

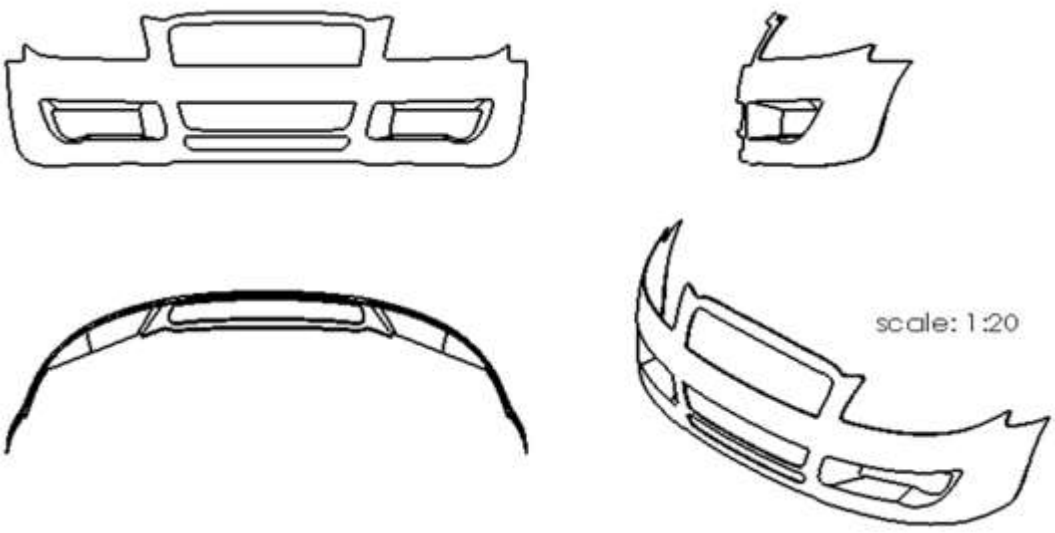

Figure 22. 2D drawing of the front bumper cover

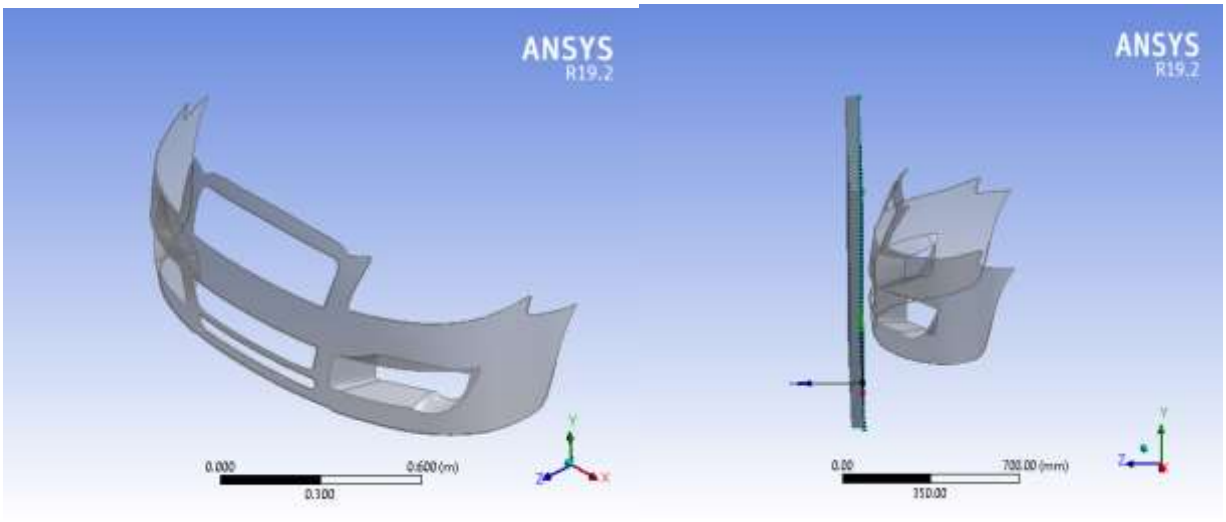

Figure 23. 3D modelling of the front bumper cover with and without impact barrier.

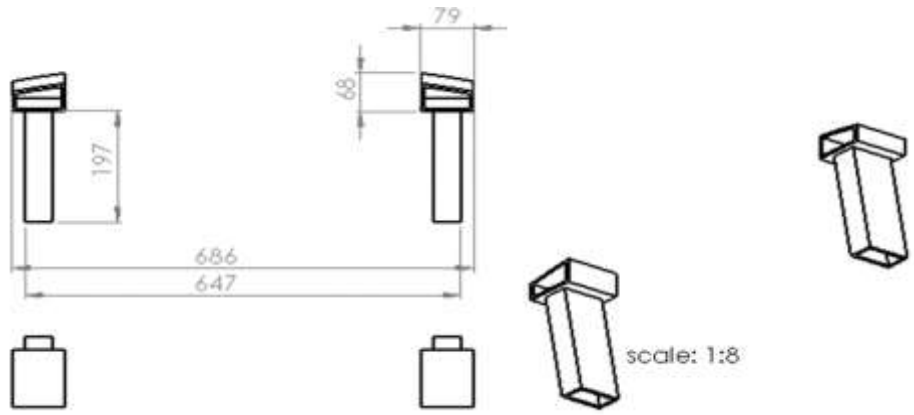

Figure 24. 2D drawing of the supporter

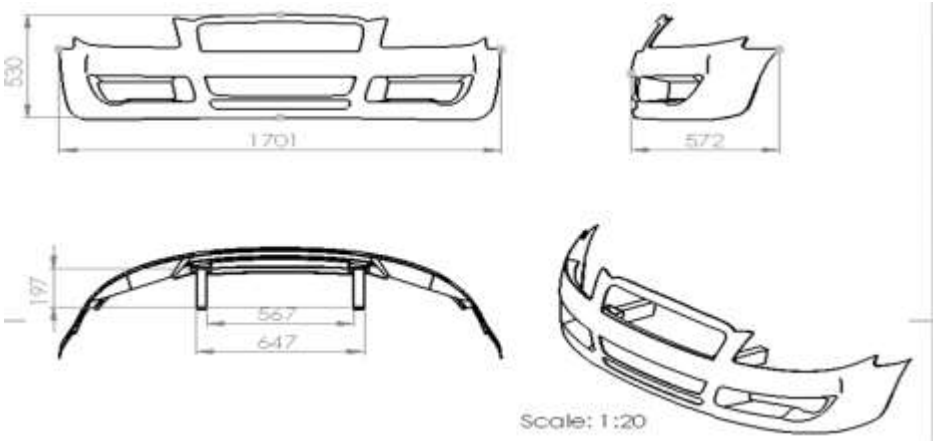

Figure 25. 2D drawing of the assembled bumper system

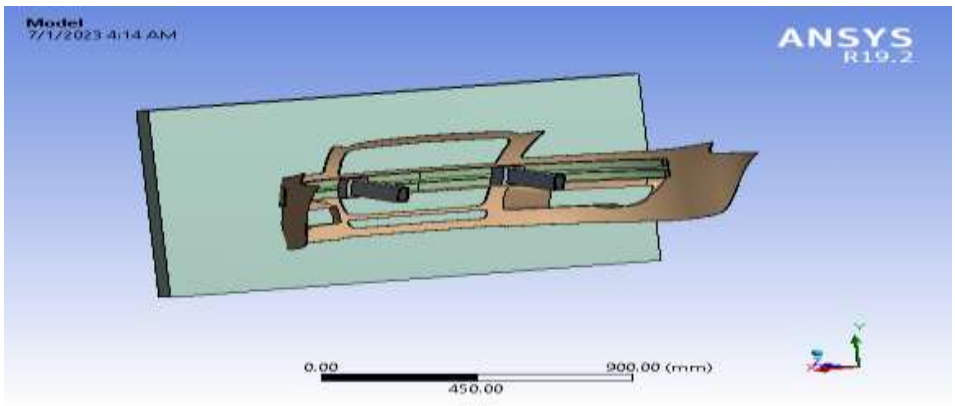

Figure 26. 3D modelling of front bumper system with impact barrier.

CHAPTER FOUR

4 FINITE ELEMENT ANALYSIS

Here are the general steps for performing a finite element impact test for a composite bumper using Ansys Workbench:

1. Import geometry: Start by importing the geometry of the composite bumper into Ansys Workbench. This can be done by either creating the geometry within Ansys or importing it from other software's.

2. Create mesh: Generate a mesh for the composite bumper geometry. The mesh should be fine enough to capture the details and features of the bumper accurately. Consider using a combination of shell elements for the outer surface and solid elements for the core material.

3. Material assignment: Assign appropriate material properties to the composite bumper.

4. Apply boundary conditions: Defining boundary conditions for the impact test typically involves fixing certain areas of the bumper to simulate mounting points or constraints, while leaving other areas free to deform.

5. Define impact load or velocity: Specify the impact load or velocity that will be applied to the bumper. This can be done by applying a concentrated pressure or velocity at a specific location on the bumper surface. The magnitude and duration of the load or velocity should be determined based on the desired impact scenario.

6. Set up analysis: Configure the analysis settings, such as the type of analysis (static, dynamic, etc.), time step size, and convergence criteria.

7. Run analysis: Run the FEA to simulate the impact condition. Ansys Workbench will solve the equations of motion and calculate the resulting deformation, stress, and strain in the composite bumper.

8. Post-processing: Analyze and interpret the results obtained from the analysis. This may involve visualizing the deformed shape, stress distribution, and energy absorption of the bumper.

Compare the results with design requirements or experimental data to evaluate the performance of the composite bumper.

4.1 Finite element analysis of the composite bumper system

4.1.1 Layered Section

Eight layers having 0.7125mm thickness are set for the cover with different fiber orientation as shown below, and the total thickness of 5.7 mm and 9.56 kg weight. However, the bumper beam and support were set to have 5.0263 kg and 4.4 kg respectively.

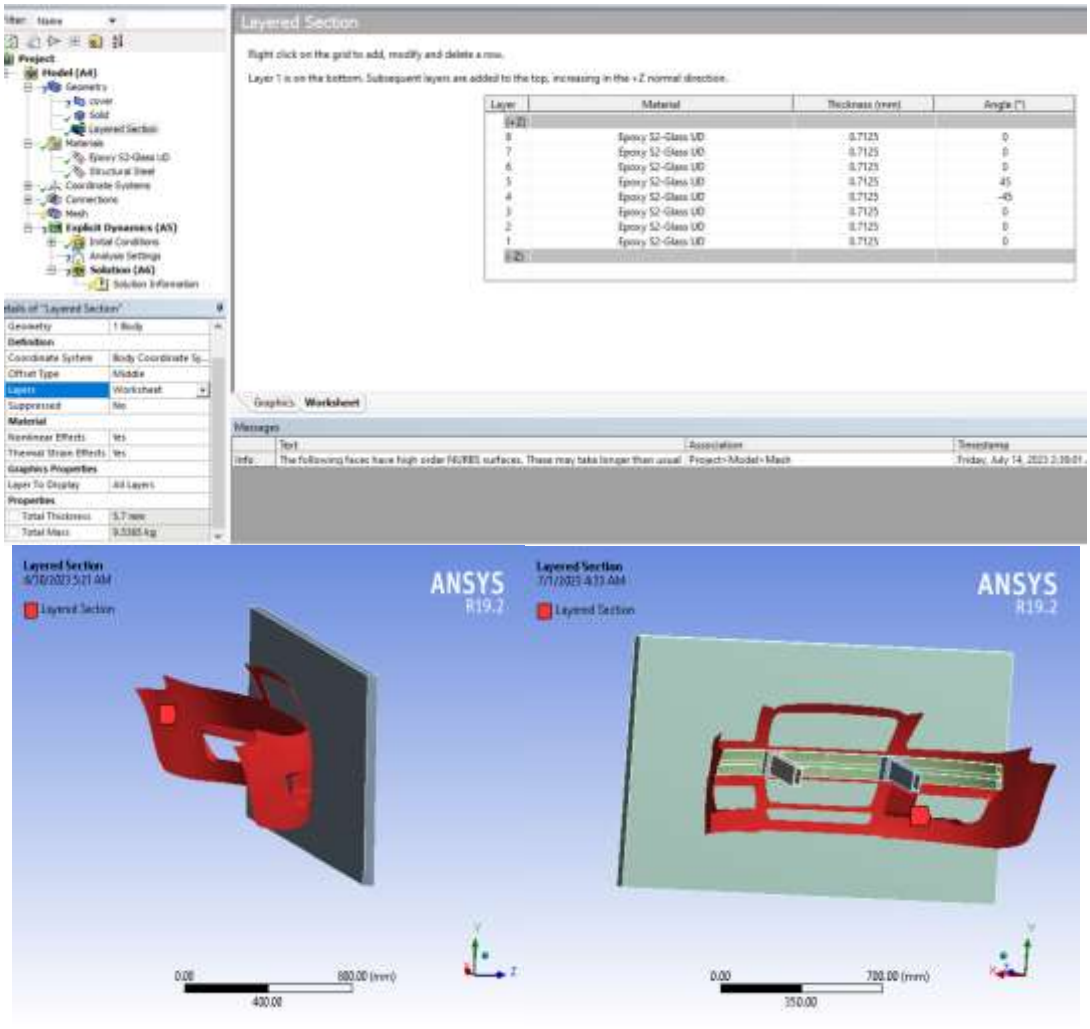

Figure 27. Layered Section of the bumper cover

4.1.2 Meshing

The ANSYS explicit dynamics tool was used to import the geometrical model created in Solid Works; the analysis began with a composite bumper. Tetrahedron components with fine mesh were used for meshing, and the mesh quality was checked.

Table 20. Mesh Detail of front bumper system

	Mesh details of front bumper system		
	Cover with barrier	Bumper beam with barrier	Assembled bumper with barrier
Element Size	5 mm	10 mm	10mm
Initial size	Active assembly	Active assembly	Active assembly
Physics preference	Explicit	Explicit	Explicit
Smoothing	High	High	High
Element type	Quadrilateral (quad/tri face)	Tetrahedron	Quad/tri for cover and Tetrahedron for beam
Material	UD S2-glass fiber reinforced epoxy with structural steel barrier	UD S2-glass fiber reinforced epoxy with structural steel barrier	UD S2-glass fiber reinforced epoxy with structural steel barrier
INFLATION			
Max layers	5		
Transition ratio	0.7	0.7	0.7
Growth rate	$0.012*10^2$	$0.012*10^2$	$0.012*10^2$
STATISTICS			
Max-nodes	820737	81384	144382
Max-elements	742524	63260	124459

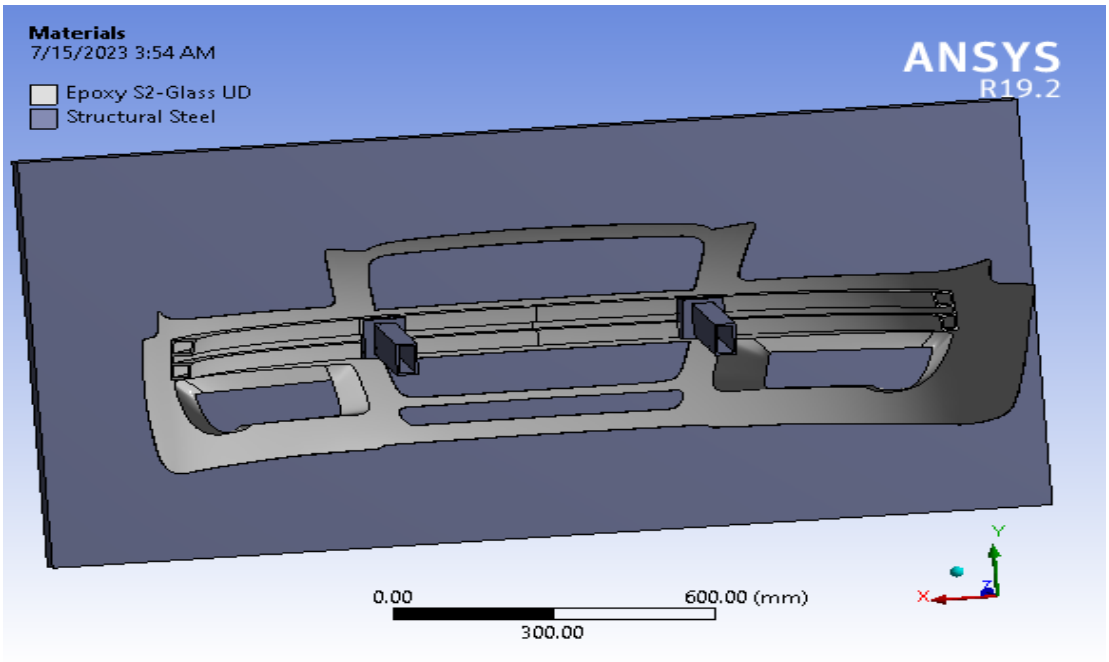

Figure 28. Material assignment of bumper system and barrier

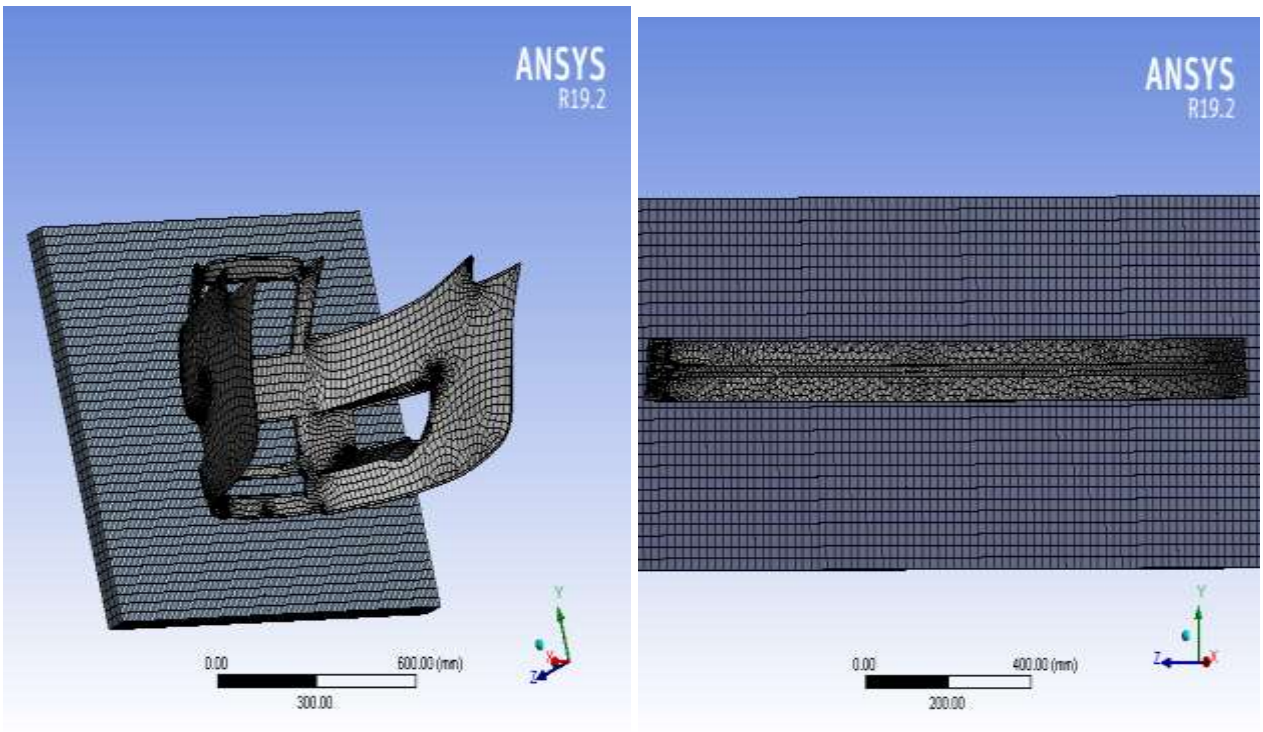

Figure 29. Meshing of cover and beam with the barrier

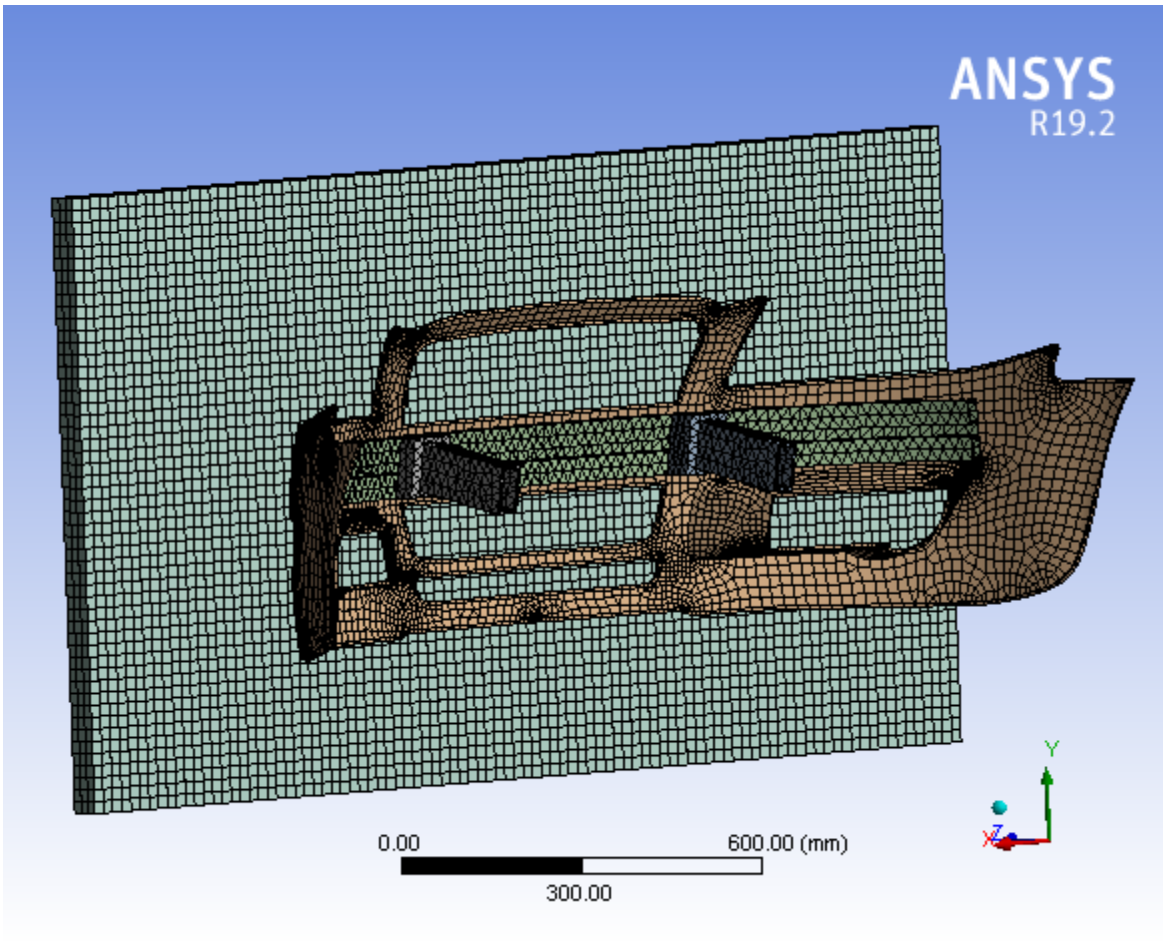

Figure 30. Meshing of bumper system with the barrier

4.1.3 Boundary conditions

The boundary conditions, which are fixed support and displacements, were placed at the barrier and a car bumper on a vehicle body-mounted location. The impact barrier was fixed at each of four faces in all cases. Displacement was added as a boundary condition for the cover part at its edges in all tasks along the y direction as shown in the figure 31. Displacement was added as a boundary condition for the bumper beam at both ends along the y direction, as shown in figure 32. Displacement was added in the overall assembly part, the bumper system, in all its directions at both ends of the support and all edges of the cover along the y direction, as shown in figure 33.

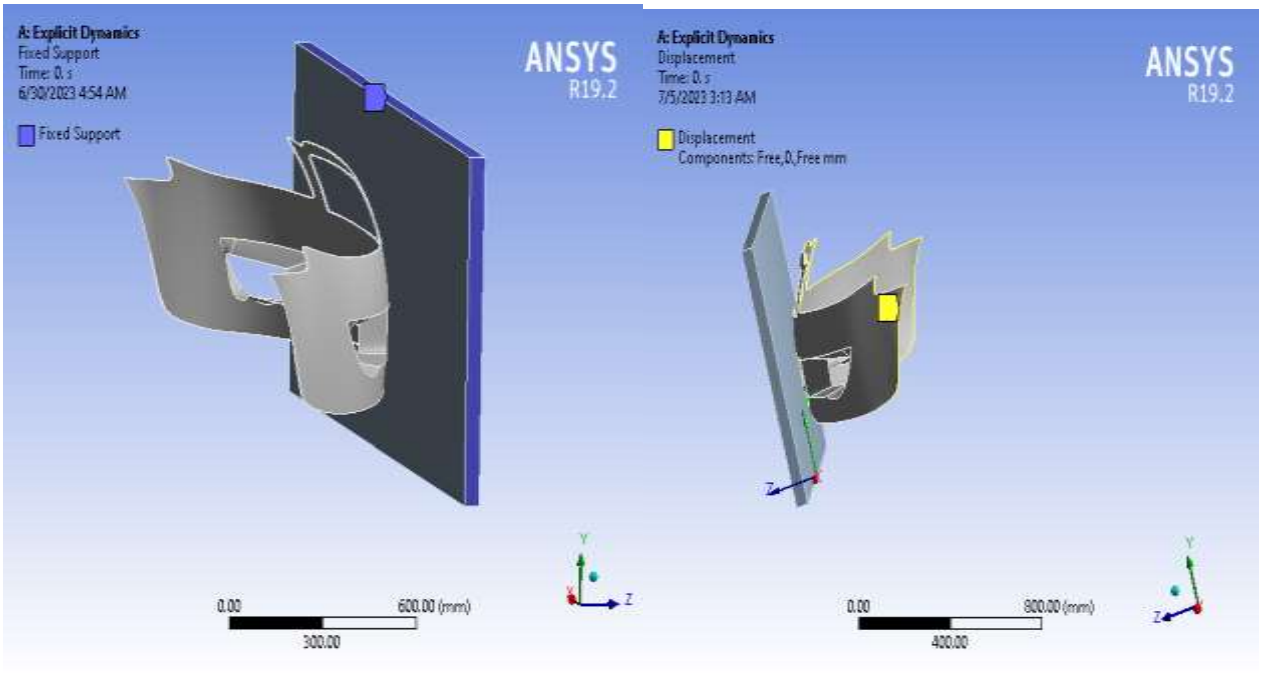

Figure 31. Displacement of the cover and fix support of the impact barrier

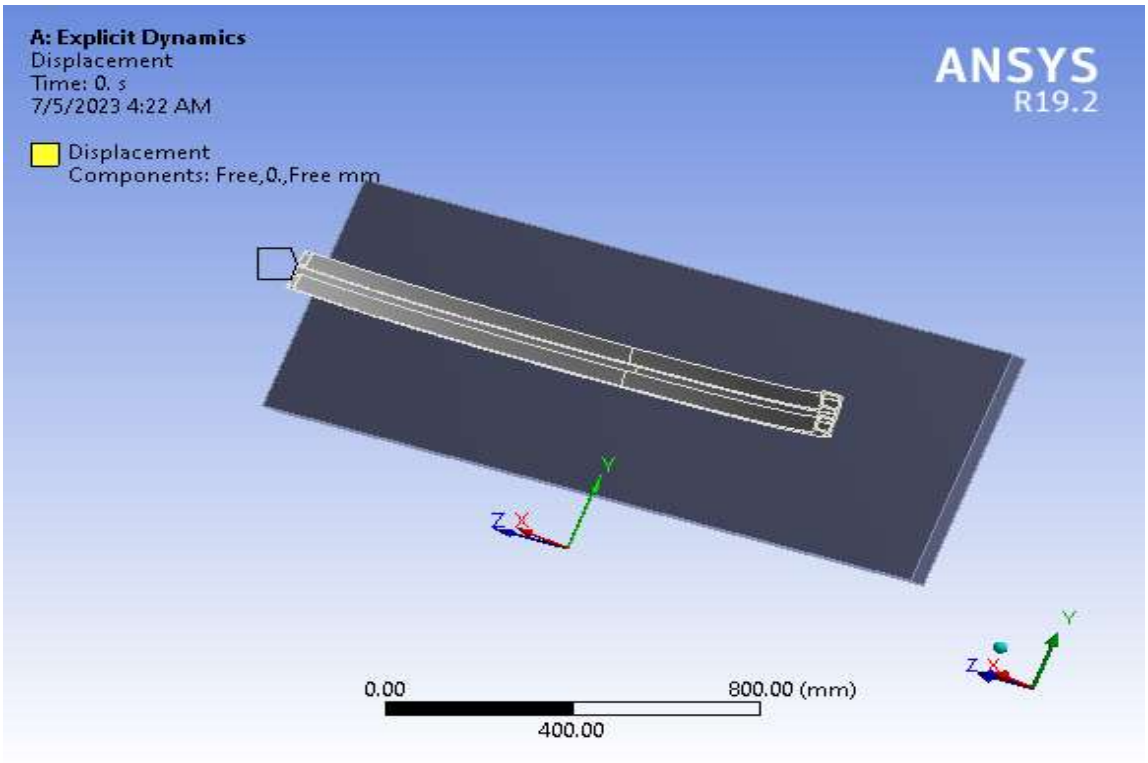

Figure 32. Displacement of the bumper beam

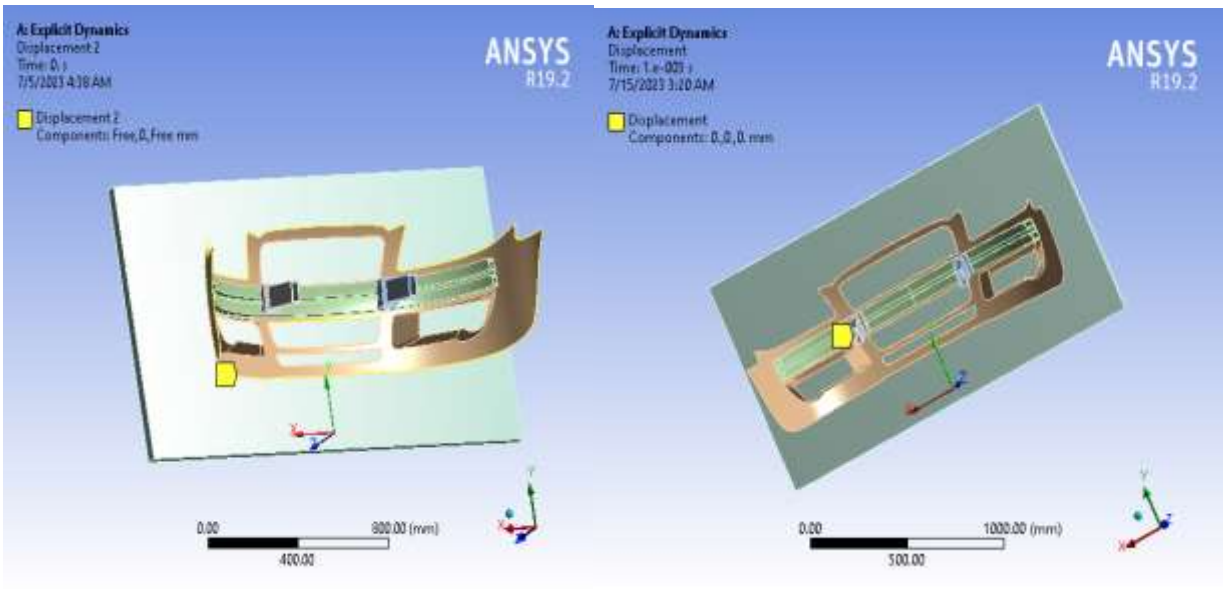

Figure 33. Displacement of the bumper system

4.1.4 Impact velocity

In this work, the impact velocity of the moving car towards the barrier was added to the initial condition of explicit dynamics at the assembled bumper along the z direction, as shown in figure 34.

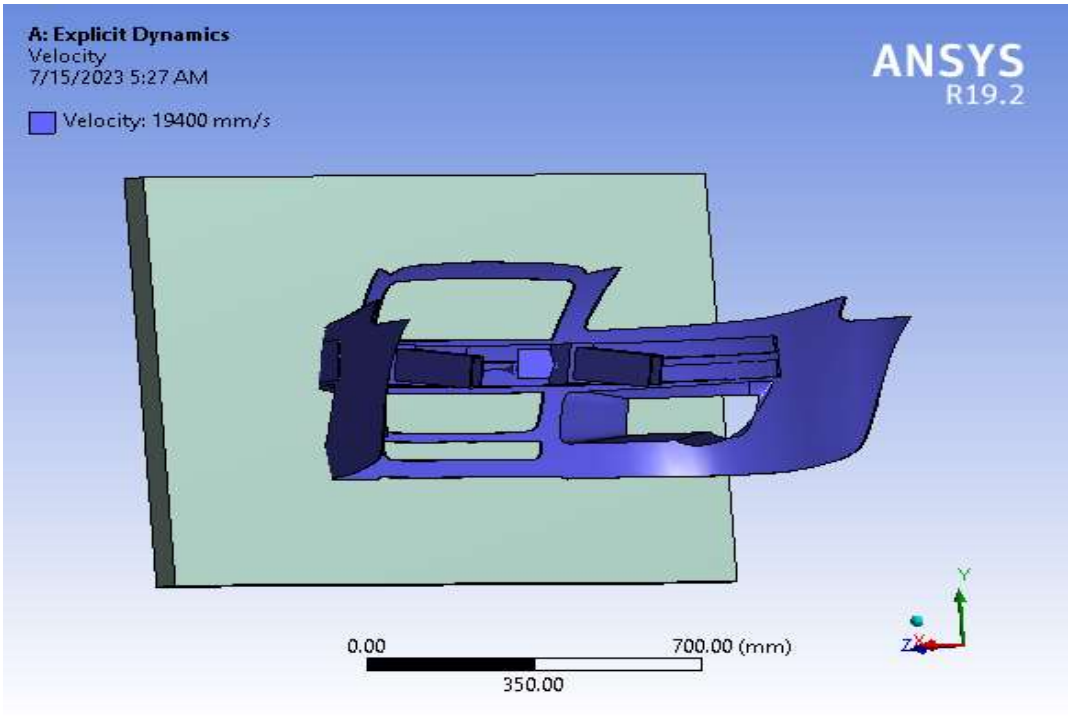

Figure 34. Impact velocity of assemble

4.1.5 General analysis setting

After defining all the necessary conditions, the next step to performing a finite-element bumper impact test is configuring the analysis settings, such as the type of analysis (static, dynamic, etc.), time step size, and number of cycles. As shown in table 21, the analysis settings for all parts were defined accordingly.

Table 21. Analysis of settings

Analysis of settings	Bumper parts		
	Cover	Beam	Assembled
	Control steps		
Max number of steps	*1*	*1*	*1*
Current step numbers	*1*	*1*	*1*
Load step types	*Explicit time integration*		
Ending time		*0.001*	*0.001*
Resume from cycle	*0*	*0*	*0*
Max number of cycles	10^7	10^7	10^7
Max energy error	*0.1*	*0.1*	*0.1*
Initial step time	*Program controlled*	*Program controlled*	*Program controlled*
Time step safety of factor	*0.9*	*0.9*	*0.9*
Characteristic dimension	*Diagonals*	*Diagonals*	*Diagonals*
Automatic mass scaling	*No*	*No*	*No*

CHAPTER FIVE

5 RESULT AND DISCUSSION

5.1 Epoxy S-2 Glass Fiber UD bumper beam results

A. Total deformation at 40 km/hr.

The resulting Epoxy S-2 glass fiber UD bumper beam alone experiences a maximum total deformation length of the bumper beam at a vehicle speed of 40 km/h was 13.576 mm, as shown in the figure 35, and When the complete bumper assembly, including the bumper beam, energy absorber, and bumper cover, is considered in the simulation, the maximum deformation decreases significantly to 1.689 mm, as shown in the figure 36.

The large difference between the deformation of the isolated bumper beam and the complete bumper system (approximately eight times lower in the full system) can be explained by the energy absorption and load distribution mechanisms of the additional bumper components. In the present study, the energy absorber is modeled as a stack of four composite plates, which act as an intermediate structural layer between the impactor and the bumper beam. During impact, these plates deform and absorb part of the kinetic energy through elastic deformation and progressive load distribution, thereby reducing the amount of force transmitted directly to the bumper beam. As a result, the structural beam experiences lower localized stresses and reduced deformation. The bumper cover also contributes to the overall stiffness of the system by increasing the contact surface area during impact, which helps distribute the impact force more uniformly across the bumper assembly. Therefore, the significantly lower deformation observed in the complete bumper system is consistent with the expected structural behavior of multi-component automotive bumper assemblies.

Based on an earlier study (Ranjithkumar and Ramesh 2015), reported a maximum deformation of 0.383 mm for an S-2 glass epoxy bumper beam subjected to a 40 km/h impact. The significantly lower deformation reported in their study may be attributed to different modeling assumptions such as beam thickness, boundary constraints, and reinforcement configuration, which strongly influence the stiffness of composite bumper structures.

Another analysis of composite bumper beams show that deformation values can vary widely depending on design parameters. (Neelima, Rao et al. 2016) investigated S-2 glass epoxy bumper beams at 8 km/h impact velocity and reported 26.86 mm deformation. In the same investigation, variations in structural parameters such as passenger load and beam thickness resulted in deformation values ranging from approximately 10.19 mm to 12.59 mm for different operating conditions.

Therefore, considering the variations reported in the literature (approximately 10–26 mm deformation under different conditions) and the influence of structural parameters such as laminate thickness, boundary conditions, and energy-absorbing components, the deformation of 13.576 mm obtained in the present study falls within a realistic and acceptable range for composite bumper beam structures and is quite plausible and even conservative. Therefore, that deformation length of 13.576 mm is quite plausible and even conservative, depending on design and failure mode.

Additionally, when the complete bumper assembly is considered including the bumper beam, stacked composite energy absorber plates, and bumper cover the deformation reduces to 1.689 mm, demonstrating the load-sharing and energy-absorbing capability of the multi-component bumper system.

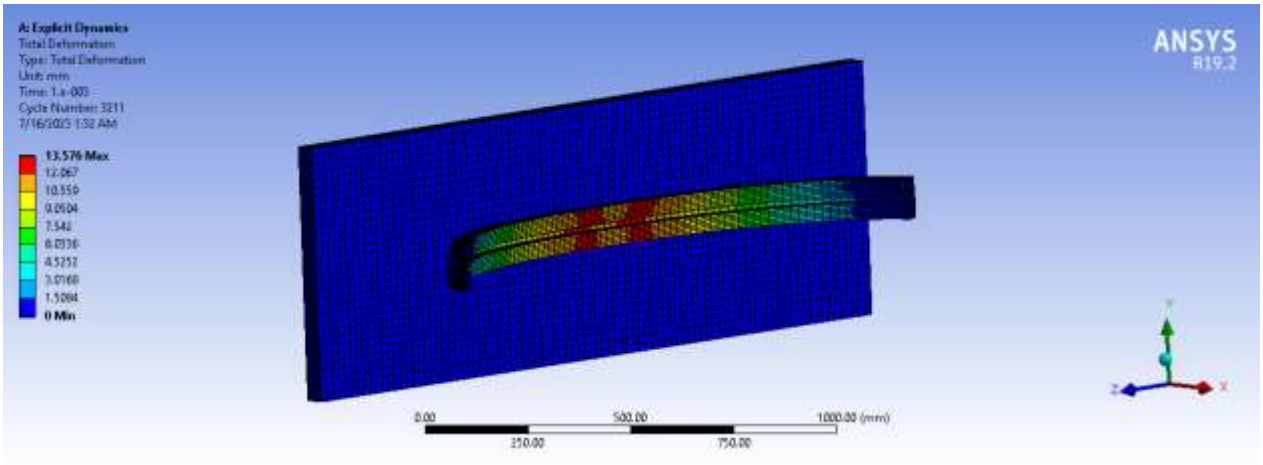

Figure 35. Bumper beam total deformation length

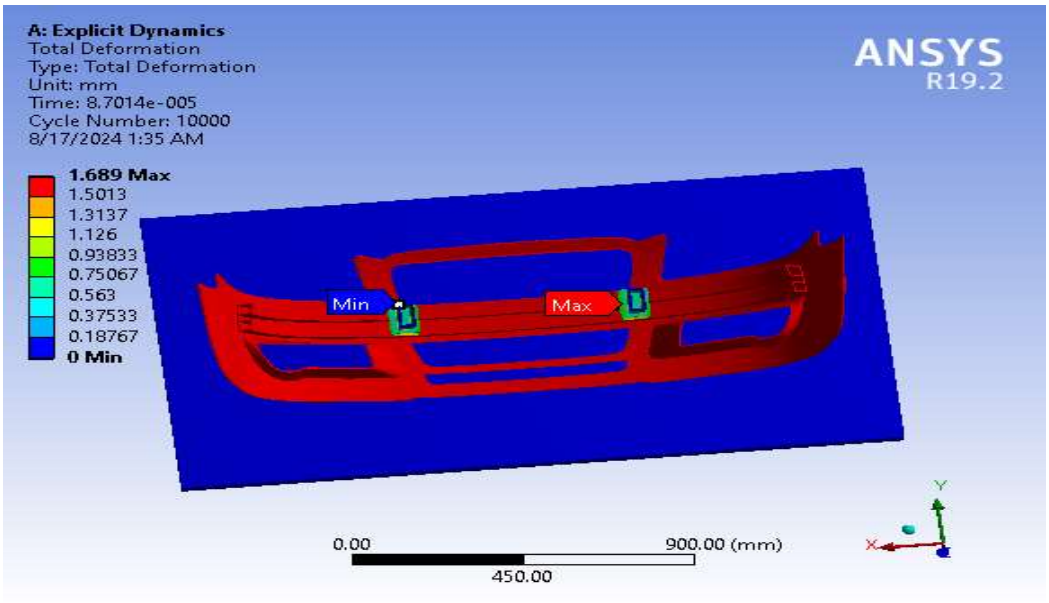

Figure 36. Bumper system total deformation length

B. Equivalent (Von –Mises) stress at 40 km/hr.

The equivalent (von-mises) stress in the S-2 glass fiber reinforced epoxy bumper at the vehicle speed of 40 km/h is 1024.8 MPa, as shown in figure 37. A comparison with published literature shows that similar stress levels have been reported for glass-fiber-reinforced composite bumper systems under impact conditions. According to the recent review (Du, Li et al. 2023), S2 glass fiber reinforced epoxy composites in low-speed collisions (30 km/h) exhibit a stress value of approximately 727.15 MPa. The higher stress value observed in the present study (1024.8 MPa) can be attributed primarily to the higher impact velocity of 40 km/h, since impact stress generally increases with impact energy according to the kinetic energy relation. The increased kinetic energy at higher velocity leads to larger contact forces and consequently higher stresses within the structural components.

A further comparison was made with traditional metallic bumper materials. The study by (Hosseinzadeh, Shokrieh et al. 2005) revealed that the conventional bumper materials that are steel and aluminum were tested at 40 km/h impact simulation, and their maximum stress value were 850 MPa and 700 MPa, respectively. Compared with these metallic materials, the higher stress value observed in the present composite bumper beam does not necessarily indicate poorer performance. Composite materials such as S-2 glass epoxy typically possess higher strength-to-weight ratios and different stress distribution characteristics due to their anisotropic fiber-

reinforced structure. The fibers carry a large portion of the load along their orientation direction, which can lead to higher localized stresses while still maintaining structural integrity.

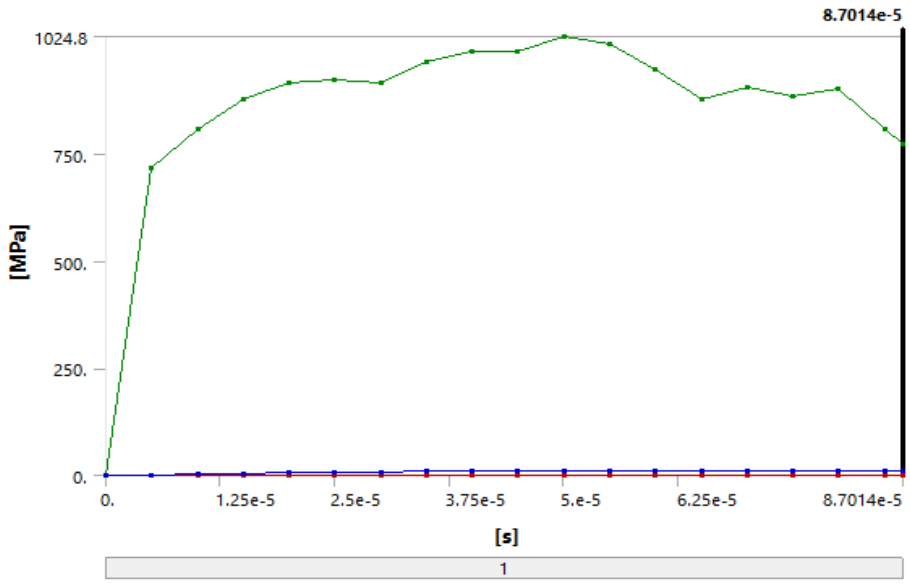

Figure 37. Equivalent(von-mises) stress of the bumper system

Although Von Mises stress is traditionally used for isotropic metallic materials, it is still commonly reported in composite impact simulations as a general scalar indicator of stress concentration and overall structural response within the finite element model. In composite structures, Von Mises stress does not represent the actual failure criterion but is useful for identifying regions of high stress distribution within the laminate during impact loading. More advanced composite-specific criteria such as Tsai–Wu or Hashin are typically used for predicting failure; however, Von Mises stress remains a useful comparative parameter for evaluating global structural behavior in crash simulations.

C. Equivalent (Von –Mises) strain at 40 km/hr.

At a vehicle, speed of 40 km/h the equivalent (von mises) strain is 0.0062 mm/mm as shown in the figure 38. This strain value indicates that the composite laminate experiences relatively small deformation compared with its allowable strain capacity, suggesting that the structure remains within the elastic deformation range during the impact event. Fiber-reinforced polymer composites such as S-2 glass epoxy generally exhibit high stiffness due to the reinforcing fibers, which limits the magnitude of strain even when the structure is subjected to relatively high stress levels.

The obtained strain result is consistent with values reported in previous numerical studies of composite bumper structures. For example (Habtamu 2017) reported an elastic strain value of approximately 0.0067 mm/mm in a finite element analysis of a bumper system subjected to impact loading. The close agreement between the strain value reported in that study and the present result (0.0062 mm/mm) indicates that both results fall within the same order of magnitude, confirming the reliability of the present simulation.

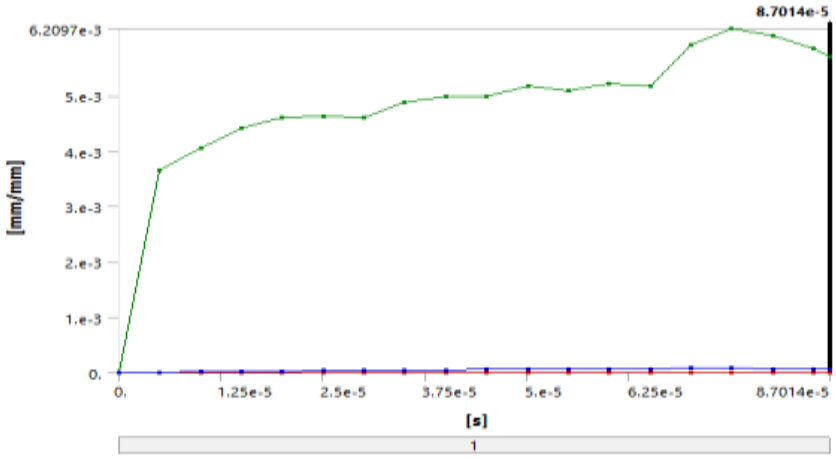

Figure 38. Equivalent Elastic Strain of bumper system

Generally, The relatively high stress but low strain response observed in this study reflects the stiff yet elastic nature of the S-2 glass fiber reinforced epoxy composite. The reinforcing glass fibers provide significant stiffness and strength, which allows the material to withstand high stresses while undergoing only limited elastic deformation. This behavior is typical of fiber-reinforced composites and contributes to their suitability for automotive crashworthy structures

such as bumper beams, where high load-carrying capacity and controlled deformation are required for effective energy absorption.

D. Internal energy at 40 km/hr.

The energy absorbed by the bumper system is the portion of that the initial energy gets dissipated through plastic deformation or through energy-absorbing materials that is not transmitted to the rest of the vehicle. This energy is evaluated to get minimal damage to vehicle parts, protecting occupants and reducing the repair costs. During the bumper impact the initial kinetic energy is partially or fully converted to other forms of energy mainly, to internal energy.

In the present simulation, the bumper beam of the Toyota sedan model impacts a rigid barrier at a velocity of 40 km/h (11.11 m/s). The initial kinetic energy associated with the impacting mass is converted primarily into internal energy within the bumper components, including the bumper beam and the stacked composite energy-absorbing plates.

The numerical results show that the total internal energy absorbed by the complete bumper system is 865 J during the impact event. Based on the combined weight of the bumper beam and the supporting energy-absorbing plates, the specific energy absorption (SEA) of the structure is calculated as 86.5 J per unit structural mass. This distinction clarifies that 865 J represents the total energy absorbed by the system, whereas 86.5 J represents the energy absorption efficiency normalized by structural weight, which is commonly used to compare crashworthiness performance across different bumper designs.

To evaluate the effectiveness of the present design, the obtained results were compared with previously published studies. The study by (Mohammadi, Ahmad et al. 2022) on lightweight glass-fiber-reinforced polymer (GFRP) bumper concepts reported specific energy absorption values ranging from approximately 41.2 J to 96.5 J for bumper structures subjected to impact loading. The specific energy absorption (SEA) value of 86.5 J obtained in the present study falls within this reported range, indicating good agreement with previously published GFRP bumper designs.

Additional comparisons can be made with studies on metallic bumper systems. For example, investigations by (Hosseinzadeh, Shokrieh et al. 2005) showed that steel and aluminum bumper

beams absorb significant impact energy but often at the expense of higher structural weight. Composite bumper structures, particularly those reinforced with glass fibers, generally demonstrate higher specific energy absorption due to their favorable strength-to-weight ratio.

Similarly, studies on glass-fiber-reinforced composite crash structures reported by (Wiggenraad, Zhang et al. 1999) indicate that GFRP automotive structural components typically achieve specific energy absorption values in the range of approximately 50–100 J/kg, depending on laminate configuration and geometry. The value obtained in the present study (86.5 J/kg equivalent) lies within this range, further supporting the validity of the numerical results.

Overall, the results demonstrate that the S-2 glass fiber reinforced epoxy bumper system effectively converts the initial impact kinetic energy into internal energy through controlled deformation, thereby improving crash energy management. The obtained energy absorption performance is consistent with the ranges reported in the literature for GFRP automotive bumper structures, indicating that the proposed composite bumper design provides competitive crashworthiness performance while maintaining a lightweight structural configuration.

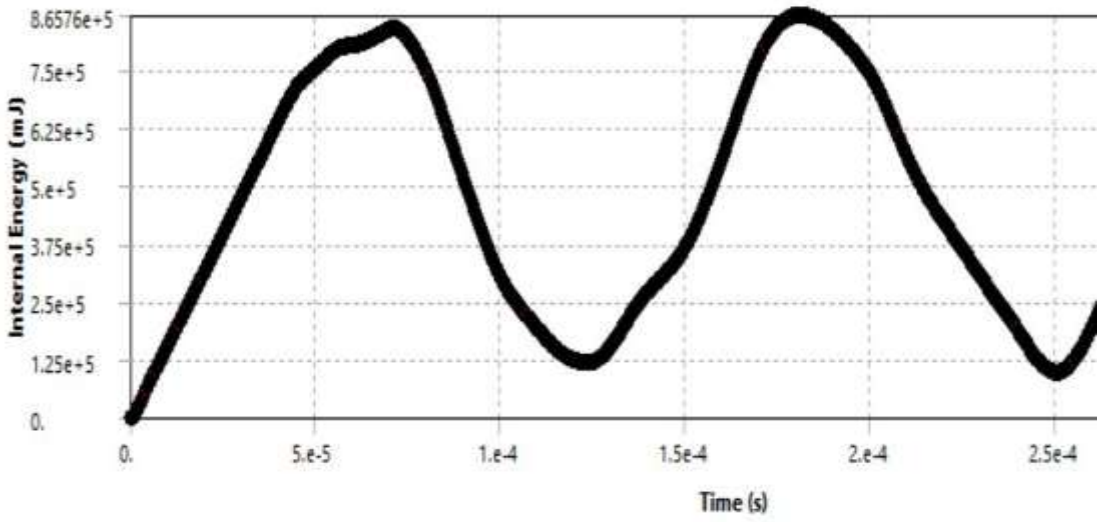

Figure 39. Internal energy of Epoxy S-2 Glass Fiber bumper material.

Description of Energy Absorption Level

In the present simulation, the bumper beam of the Toyota sedan model impacts a rigid barrier at a velocity of 40 km/h (11.11 m/s) with an effective impact mass of 19 kg. Based on the classical kinetic energy equation (eq 53), the initial kinetic energy of the beam and support is approximately 1173 J. During the collision event, a portion of this kinetic energy is converted into internal energy within the bumper components, including the S-2 glass fiber reinforced epoxy bumper beam and the stacked composite energy-absorbing plates. The numerical results indicate that the total internal energy absorbed by the bumper system is 865 J as shown in the figure 39, corresponding to approximately 73.8% of the initial kinetic energy being dissipated through structural deformation of the bumper components. To validate the results, comparisons were made with other component-level bumper impact studies using similar low-mass impactors.. Most studies on composite bumper beams with impactor masses of 15–25 kg reported energy absorption in the range of 600–900 J, with efficiency between 65–75%. In (Hambali, Kasim et al. 2022), a bumper beam impacted by a 20 kg striker absorbed about 570 J, corresponding to 55–60% of the initial energy. These comparisons indicate that the energy absorption and dissipation in the present study are well within the range reported in the literature, confirming the consistency and validity of the simulation results for a bumper system subjected to localized impacts.

CHPTER SIX

6 CONCLUSION AND RECOMMENDATIONS

6.1 Conclusion

An analytical hierarchy process (AHP) approach was used and systematically evaluated; the result confirmed the glass fiber epoxy composite bumper had superior capability to absorb impact energy and performance compared to the other candidates.

The total internal energy absorbed by the complete bumper system was 865 J, corresponding to a specific energy absorption (SEA) of 86.5 J/kg. This represents approximately 73.8% of the initial kinetic energy (1173 J) being dissipated through structural deformation, which is well within the range reported in the literature for composite bumper structures (41.2–96.5 J). The results confirm that the Epoxy S-2 Glass Fiber bumper system efficiently converts impact kinetic energy into internal energy, thereby protecting the vehicle structure and occupants while maintaining a lightweight design.

The bumper beam experienced a maximum total deformation of 13.576 mm, which is consistent with previously reported values for S-2 glass epoxy composite beams under similar conditions. When integrated into the full bumper assembly, including the stacked composite energy absorber plates and bumper cover, the deformation decreased substantially to 1.689 mm. This significant reduction illustrates the load-sharing and energy-distributing effects of the multi-component bumper system, confirming that combining composite beams with intermediate energy-absorbing layers enhances overall bumper performance.

The maximum stress observed in the traditional steel and aluminum bumpers was 850 and 700 MPa respectively, at vehicle speeds of 40 kmph. In contrast, the new Epoxy S-2 Glass Fiber bumper system experienced a significantly higher stress value of 1024.pa under the same speed conditions.

This higher stress indicates that the composite bumper can withstand larger localized loads due to its anisotropic fiber-reinforced structure, without compromising structural integrity.

The observed equivalent strain of 0.0062 mm/mm remained within the elastic range, with minimal delamination or progressive failure, demonstrating the stiff yet resilient behavior of the S-2 glass fiber epoxy laminate.

The study concludes that the Epoxy S-2 Glass Fiber bumper design offers superior protection, and it can effectively withstand the impact forces encountered at speed of 40km/h. The combination of high specific energy absorption, low deformation, and elastic response confirms the potential of these materials for next-generation bumper systems.

6.2 Recommendation

On the basis of this study, the following recommendations and prospects for future work were presented.

- For more accurate assessment safety, it is recommended to include side collusion scenarios in addition to frontal collisions.
- Incorporating a full vehicle model impact test in the simulation can provide more realistic results.
- It is advisable for researchers to design a control system and integrate it with the bumper.
- To get optimal absorption energy, it is advisable to use hybrid materials, which combine glass fibers with natural fibers, and foam with different layer arrangements.
- Experimental validation and cost performance analysis are suggested to further strengthen the material selection process and support for industrial adoption.
- Overall, it is recommended to use an Epoxy S-2 Glass Fiber bumper, as the literatures shows that a conventional bumper absorbs less energy compared to an polymer based bumper.

REFERENCES

Abd-Ali, N. K. and A. R. J. K. J. o. E. Madeh (2016). "Effect of fiber orientation angles on mechanical behavior of car bumper composite." **7**(3): 27-37.

Abhemanyu, P., et al. (2019). Characterization of natural fiber reinforced polymer composites. AIP conference proceedings, AIP Publishing.

Abrate, S. (2011). Impact engineering of composite structures, Springer Science & Business Media.

Ahmed, M. N., et al. (2013). "A study on effect of variation of thickness on tensile properties of hybrid polymer composites (glassfibre-carbonfibre-graphite) and GFRP composites." **3**(4): 2015-2024.

Ariff, H., et al. (2008). "Use of analytical hierarchy process (AHP) for selecting the best design concept." 1â€“18-11â€“18.

Chawla, K. K. (2012). Composite materials: science and engineering, Springer Science & Business Media.

Cheon, S. S. and J. H. J. C. s. Choi (1995). "Development of the composite bumper beam for passenger cars." **32**(1-4): 491-499.

da Silva, A. A. X., et al. (2022). "Influence of hybridization on the mechanical and dynamic mechanical properties of aramid/S2-glass hybrid laminates." **32**: 104021.

Daniel, I. M., et al. (1994). Engineering mechanics of composite materials, Oxford university press New York.

Davallo, M., et al. (2010). "Effects of laminate thickness and ply-stacking sequence on the mechanical properties and failure mechanism of unidirectional glass-polyester composites." **2**(4): 2118-2124.

Dhakal, H. N., et al. (2007). "Effect of water absorption on the mechanical properties of hemp fibre reinforced unsaturated polyester composites." **67**(7-8): 1674-1683.

Dixit, Y., et al. (2017). Crashworthiness performance of carbon fiber composite (CFC) vehicle front bumper crush can (FBCC) assemblies subjected to high speed 40% offset frontal impact. ASME International Mechanical Engineering Congress and Exposition, American Society of Mechanical Engineers.

Du, B., et al. (2023). "Application of lightweight structure in automobile bumper beam: a review." **16**(3): 967.

El-Wazery, M., et al. (2017). "Mechanical properties of glass fiber reinforced polyester composites." **14**(3): 121-131.

Eshetu, B. J. B. D. U. (2019). "Analysis of the regulation of key risk factors to road traffic accident in Ethiopia and challenges for enforcement." **10**: 201.

Fong, L. and S. Advani (1998). Resin Transfer Molding, Handbook of Composites, edited by ST Peters, Chapman & Hall.

Goez, J. and M. Rexhepi (2018). "Modeling of Front Bumper system with emphasis on lightweight and low cost: A product development project at Volvo Cars."

Habtamu, M. J. A. A. U. (2017). "Automobile Bumper Beam Analysis to Improve Energy Absorption."

Halpin, J. C. (1969). Effects of environmental factors on composite materials.

Hambali, A., et al. (2022). "Simulation Study on Structure Bumper Beam using Finite Element Analysis." **15**.

Hosseinzadeh, R., et al. (2005). "Parametric study of automotive composite bumper beams subjected to low-velocity impacts." **68**(4): 419-427.

Ihimekpen, N., et al. (2017). "The use of AHP (analytical hierarchy process) as multi criteria decision tool for the selection of best water supply source for Benin City." **1**(1): 169-176.

Jacob, A. B. and O. Arunkumar (2016). Improving the crashworthiness of an automobile bumper. International conference on emerging trends in engineering and management.

Madarapu, C. V. K. J. A. and A. A. V. Mohan "FE Analysis on Vehicle Bumper Using Different Materials and Speeds."

Marzbanrad, J., et al. (2009). "Design and analysis of an automotive bumper beam in low-speed frontal crashes." **47**(8-9): 902-911.

Mohammadi, H., et al. (2022). "Lightweight glass fiber-reinforced polymer composite for automotive bumper applications: a review." **15**(1): 193.

MOTGI, N. S., et al. ""“DESIGN IMPROVEMENT IN FRONT BUMPER OF A PASSENGER CAR USING IMPACT ANALYSIS”-A REVIEW."

Nachippan, N. M., et al. (2021). "Numerical analysis of natural fiber reinforced composite bumper." **46**: 3817-3823.

Neelima, V., et al. (2016). "Design and Analysis of Bumper Beam with Composite Materials." **3**: 253-259.

Norman, D. A. and R. E. J. J. o. a. p. s. Robertson (2003). "The effect of fiber orientation on the toughening of short fiber-reinforced polymers." **90**(10): 2740-2751.

Olorunnishola, A. and E. J. I. J. M. C. E. Adubi (2018). "A comparative analysis of a blend of natural jute and glass fibers with synthetic glass fibers composites as car bumper materials." **15**: 67-71.

Osokoya, O. J. I. J. o. A. C. (2017). "An evaluation of polymer composites for car bumper beam." **3**(1): 44-60.

Prabhu, T. P., et al. (2018). "Ideation Selection of a New Product Using Fuzzy Multi Criteria Decision Making and Promethee." **10**(7).

Priyatam, P. D. and V. J. I. R. J. E. T. Madhav (2018). "Impact analysis and Material optimization of a front bumper in a heavy vehicle." **5**.

Ranjithkumar, R. and J. J. J. C. P. S. Ramesh (2015). "Modelling and analysis of a car bumper using various materials by FEA software." **2015**: 294-298.

Rathnakar, G., et al. (2013). "Fibre orientation and its influence on the flexural strength of glass fibre and graphite fibre reinforced polymer composites." **2**(3): 548-552.

Sonawane, C. R. and A. L. J. J. o. T. I. o. E. S. C. Shelar (2018). "Strength enhancement of car front bumper for slow speed impact by FEA method as per IIHS regulation." **99**(5): 599-606.

Srivastava, J. P., et al. (2022). "Introduction to glass fiber-based composites and structures." 1-16.

Stucki, S. L., et al. (1995). "NHTSA's improved frontal protection research program." 826-838.

Wang, T. and Y. J. A. i. M. E. Li (2015). "Design and analysis of automotive carbon fiber composite bumper beam based on finite element analysis." **7**(6): 1687814015589561.

Wiggenraad, J., et al. (1999). "Impact damage prediction and failure analysis of heavily loaded, blade-stiffened composite wing panels." **45**(2): 81-103.

Xiao, Z., et al. (2015). "Crashworthiness design for functionally graded foam-filled bumper beam." **85**: 81-95.

Yarlagaddaa, J. and M. J. M. T. P. Ramakrishna (2019). "Fabrication and characterization of S glass hybrid composites for Tie rods of aircraft." **19**: 2622-2626.

Zhang, N., et al. (2019). "Functionally graded materials: an overview of stability, buckling, and free vibration analysis." **2019**(1): 1354150.

Zhu, G., et al. (2017). "Design optimisation of composite bumper beam with variable cross-sections for automotive vehicle." **22**(4): 365-376.

Appendix

ALTERNATIVES ON DESIGN CONCEPT

A-1

Criteria	Energy absorption	Performance	Manufacturing method	Cost	Availability	Total row	Priority vector
Energy absorption	1	2	3	2	3	1.867	0.373
Performance	1/2	1	2	1	2	1.06	0.21
Manufacturing method	1/3	1/2	1	1	2	0.75	0.15
Cost	1/2	1	1	1	2	0.912	0.182
Availability	1/3	1/2	1/2	1/2	1	0.487	0.097

For $R_I = 1.12, \lambda_{max} = 5.075, C_I = 0.019$ and $C_R = 0.0168$

A-2

Criteria	Energy absorption	Performance	Manufacturing method	Cost	Availability	Total row	Priority vector
Energy absorption	1	3	5	3	5	2.305	0.46
Performance	1/3	1	3	1	3	0.985	0.2
Manufacturing method	1/5	1/3	1	1	3	0.61	0.12
Cost	1/3	1	1	1	3	0.792	0.158

Availability	1/5	1/3	1/3	1/3	1	0.31	0.062

For $R_I = 1.12, \lambda_{max} = 5.21, C_I = 0.052$ and $C_R = 0.046$

A-3

Criteria	Energy absorption	Performance	Manufacturing method	Cost	Availability	Total row	Priority vector
Energy absorption	1	3	5	3	5	2.305	0.46
Performance	1/3	1	3	1	3	0.985	0.2
Manufacturing method	1/5	1/3	1	1	3	0.61	0.12
Cost	1/3	1	1	1	3	0.792	0.158
Availability	1/5	1/3	1/3	1/3	1	0.31	0.062

For $R_I = 1.12, \lambda_{max} = 5.21, C_I = 0.052$ and $C_R = 0.046$

A-4

Criteria	Energy absorption	Performance	Manufacturing method	Cost	Availability	Total row	Priority vector
Energy absorption	1	3	5	3	7	2.326	0.465
Performance	1/3	1	3	1	5	1.051	0.21

Manufacturing method	1/5	1/3	1	2	3	0.692	0.138
Cost	1/3	1	1/2	1	3	0.692	0.138
Availability	1/7	1/5	1/3	1/3	1	0.24	0.048

For $R_I = 1.12, \lambda_{max} = 5.31, C_I = 0.078$ and $C_R = 0.069$

A-5

Criteria	Energy absorption	Performance	Manufacturing method	Cost	Availability	Total row	Priority vector
Energy absorption	1	4	6	4	7	2.567	0.513
Performance	1/4	1	3	1	5	0.951	0.19
Manufacturing method	1/6	1/3	1	2	3	0.633	0.13
Cost	1/4	1	1/2	1	3	0.615	0.123
Availability	1/7	1/5	1/3	1/3	1	0.233	0.047

For $R_I = 1.12, \lambda_{max} = 5.35, C_I = 0.088$ and $C_R = 0.078$

A-6

Criteria	Energy	Performanc	Manufacturin	Cos	Availabilit	Total	Priorit

	absorption	e	g method	t	y	row	y vector
Energy absorption	1	5	7	4	7	2.68	0.54
Performance	1/5	1	3	1	5	0.885	0.18
Manufacturing method	1/7	1/3	1	2	3	0.61	0.122
Cost	1/4	1	1/2	1	3	0.597	0.12
Availability	1/7	1/5	1/3	1/3	1	0.23	0.046

For $R_I = 1.12, \lambda_{max} = 5.37, C_I = 0.099$ and $C_R = 0.0884$

Materials Alternatives	**Overall priority vector**	Normalized overall priority vector (low to high ranking order)
A-6	0.264	0.145
A-5	0.295	0.164
A-4	0.295	0.1643
A-3	0.3	0.167
A-2	0.312	0.174
A-1	0.33	0.184
Total	1.796	1.000

Layered section with orientation angle

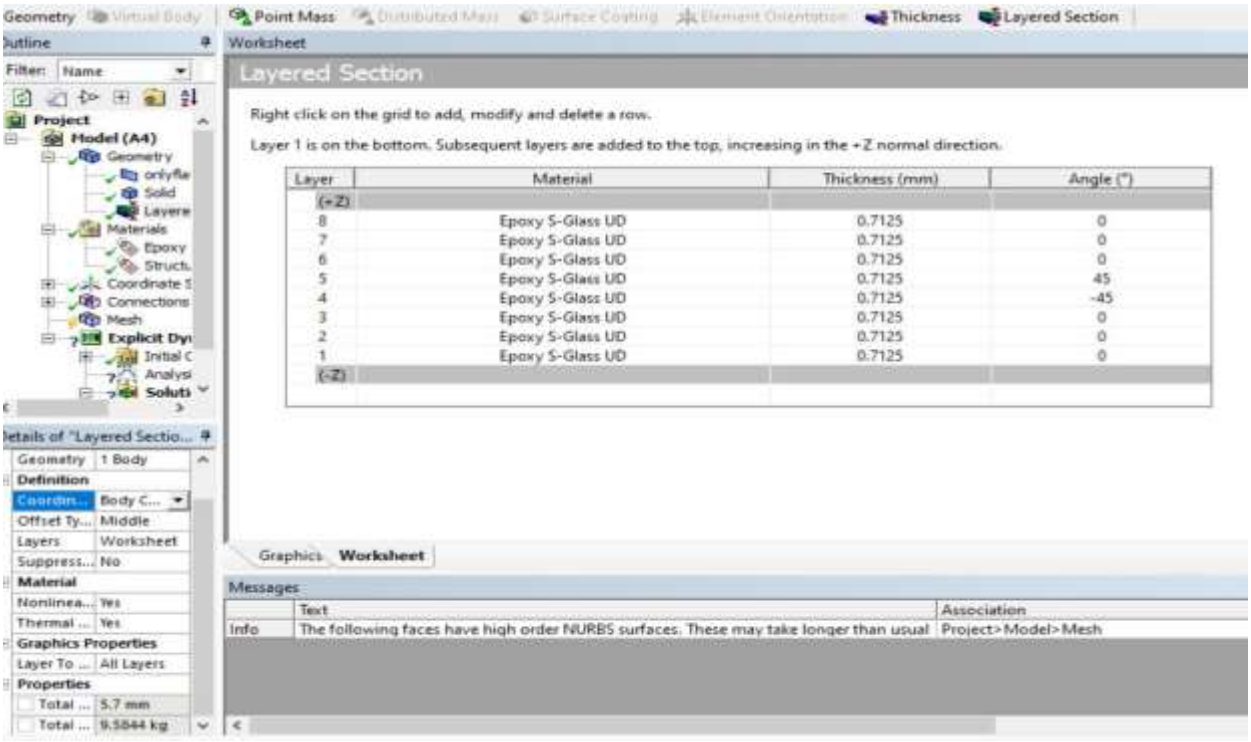

Engineering data source

Properties of Outline Row 3: Epoxy S2-Glass UD 2

	A	B	C	D	E
1	Property	Value	Unit		
2	Density	1.99	g cm^-3		
3	Orthotropic Elasticity				
4	Young's Modulus X direction	56000	MPa		
5	Young's Modulus Y direction	18000	MPa		
6	Young's Modulus Z direction	18000	MPa		
7	Poisson's Ratio XY	0.27			
8	Poisson's Ratio YZ	0.256			
9	Poisson's Ratio XZ	0.27			
10	Shear Modulus XY	7500	MPa		
11	Shear Modulus YZ	1252	MPa		
12	Shear Modulus XZ	7500	MPa		
13	Orthotropic Stress Limits				
14	Tensile X direction	1770	MPa		
15	Tensile Y direction	61.5	MPa		
16	Tensile Z direction	61.5	MPa		
17	Compressive X direction	-965	MPa		
18	Compressive Y direction	-155	MPa		
19	Compressive Z direction	-155	MPa		
20	Shear XY	113.5	MPa		
21	Shear YZ	129	MPa		
22	Shear XZ	129	MPa		
23	Orthotropic Strain Limits				
24	Tensile X direction	0.031			
25	Tensile Y direction	0.00375			
26	Tensile Z direction	0.00375			
27	Compressive X direction	-0.0145			
28	Compressive Y direction	-0.012			
29	Compressive Z direction	-0.0105			
30	Shear XY	0.0205			
31	Shear YZ	0.0182			
32	Shear XZ	0.0205			